Plant Systematics and Evolution (2021) 307:57
https://doi.org/10.1007/s00606-021-01775-y

ORIGINAL ARTICLE

Climate and coastal low-cloud dynamic in the hyperarid Atacama fog Desert and the geographic distribution of *Tillandsia landbeckii* (Bromeliaceae) dune ecosystems

Juan-Luis García[1,2] · Felipe Lobos-Roco[3,4] · Jan H. Schween[5] · Camilo del Río[1,2] · Pablo Osses[1,2] · Raimundo Vives[1,2] · Mariana Pezoa[1,2] · Alexander Siegmund[6,7] · Claudio Latorre[2,8,9] · Fernando Alfaro[9,10] · Marcus A. Koch[11,12] · Ulrich Loehnert[5]

Received: 26 March 2021 / Accepted: 5 July 2021

Abstract

Despite the extensive area covered by the coastal Atacama fog Desert (18–32° S), there is a lack of understanding of its most notorious characteristics, including fog water potential, frequency of fog presence, spatial fog gradients or fog effect in ecosystems, such as Tillandsia fields. Here we discuss new meteorological data for the foggiest season (July–August–September, JAS) in 2018 and 2019. Our meteorological stations lie between 750 and 1211 m a. s. l. at two sites within the Cordillera de la Costa in the hyperarid Atacama (20° S): Cerro Oyarbide and Alto Patache. The data show steep spatial gradients together with rapid changes in the low atmosphere linked to the advection of contrasting coastal (humid and cold) and continental (dry and warm) air masses. One main implication is that fog presence and fog water yields tend to be negatively related to both distance to the coast and elevation. Strong afternoon SW winds advect moisture inland, which take the form of fog in only about 6% of the JAS at 1211 m a. s. l., but 65% at 750 m a. s. l. on the coastal cliff. Although sporadic, long lasting fog events embrace well-mixed marine boundary layer conditions and thick fog cloud between 750 and 1211 m a. s. l. These fog events are thought to be the main source of water for the Tillandsia ecosystems and relate their geographic distribution to the lowest fog water yields recorded. Future climate trends may leave fog-dependent Tillandsia even less exposed to the already infrequent fog resulting in rapid vegetation decline.

Keywords Atacama fog Desert · Camanchaca · Marine boundary layer (MBL) · Southeast Pacific · *Tillandsia landbeckii*

Handling editor: Marcus Koch.

Contribution to "Living at its dry limits – Tillandsiales in the Atacama Desert".

✉ Juan-Luis García
jgarciab@uc.cl

1 Instituto de Geografía, Facultad de Historia, Geografía y Ciencia Política, Pontificia Universidad Católica de Chile, Santiago, Chile

2 Centro UC Desierto de Atacama, Pontificia Universidad Católica de Chile, Santiago, Chile

3 Departamento de Ingeniería Hidráulica y Ambiental, Pontificia Universidad Católica de Chile, Santiago, Chile

4 Meteorology and Air Quality Group, Wageningen University, Wageningen, The Netherlands

5 Institute for Geophysics and Meteorology, University of Cologne, Cologne, Germany

6 Heidelberg Center for the Environment and Institute for Geography, Heidelberg University, Heidelberg, Germany

7 Research Group for Earth Observation (rgeo), Department of Geography, Heidelberg University of Education, Heidelberg, Germany

8 Departamento de Ecología, Pontificia Universidad Católica de Chile, Santiago, Chile

9 Instituto de Ecología and Biodiversidad (IEB), Casilla 653, Santiago, Chile

10 GEMA Center for Genomics, Ecology and Environment, Universidad Mayor, Camino La Piramide 5750, Huechuraba, Santiago, Chile

11 Centre for Organismal Studies, Heidelberg University, 69120 Heidelberg, Germany

12 Heidelberg Center for the Environment HCE, Heidelberg University, 69120 Heidelberg, Germany

Published online: 06 September 2021

Introduction

The coastal Atacama Desert is characterized by a dynamic low-level atmospheric circulation (Rutllant et al. 2003). In its northern hyperarid sector (20° S) at about 1000 m a. s. l., the inland dry desert climate encounters the coastal moist maritime desert air masses each one embracing distinct and contrasting atmospheric characteristics (Fuenzalida 1950; Weischet 1975; Cereceda et al. 2008a). The boundary between both climates—the marine boundary layer and the continental boundary layer—was described by Weischet as a "sharp and fine bordering line" in reference to the subsidence thermal inversion base and fog cloud top contact surface (Weischet 1975, p.369). Whereas virtually no rain is recorded here, Houston and Hartley (2003) reported for the coastal towns of Arica (18.5° S): 0.9 mm/y, Iquique (20.5° S): 1.5 mm/y and Antofagasta (23.7° S): 3.1 mm/y), the maritime air masses represent a unique source of moisture in the form of frequent fog. The "Camanchaca," as it is locally named (del Río et al. 2021a), is the terrestrial expression of the off-shore stratocumulus (Sc) cloud, ubiquitous in the Southeast Pacific Ocean (Cereceda et al. 2008a; Garreaud et al. 2008; del Río et al. 2018, 2021a) (Fig. 1).

In Chile, fog is a common phenomenon along the coastal side of the N–S trending Cordillera de la Costa that spans over > 2000 km. The thermal inversion caused by pervasive

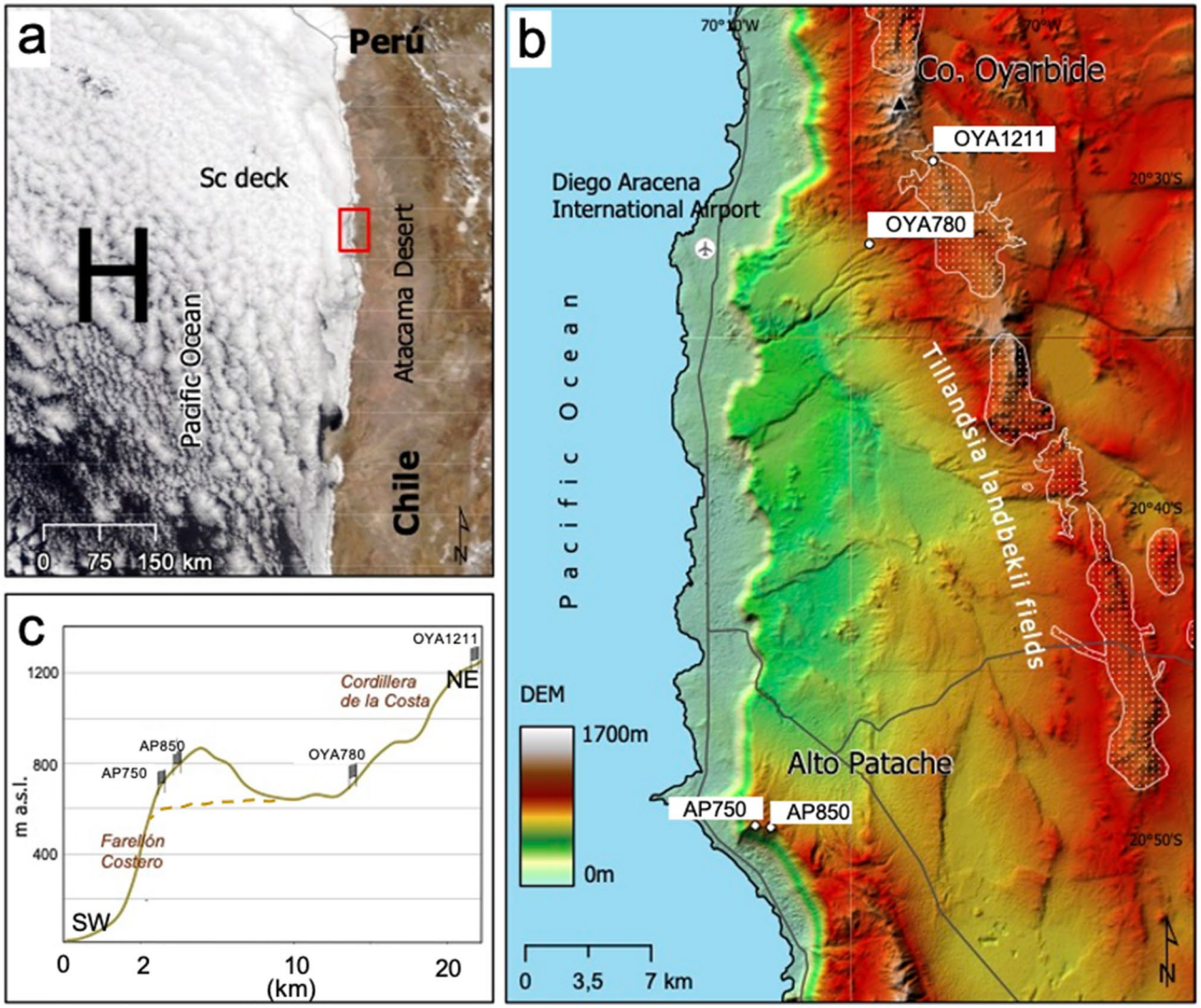

Fig. 1 Hyperarid coastal Atacama Desert. **a** Southeast Pacific Stratocumulus cloud (September 17, 2020); *H* Anticyclonic High Pressure, red box indicates location of detail map. **b** Detail of the study area including the location of the meteorological stations and the Tillandsia fields on the Cordillera de la Costa (Base map: DEM terrain data downloaded from ASF DAAC (2011)). **c** Schematic vertical SW–NE cross section of the topographic elevation and referential distance to the coastline relation of each meteorologic station. Dashed line indicate topography to the west of OYA780 before the coastal cliff

subsidence constrains the fog Sc cloud within the marine boundary layer (MBL) and the overall extent of maritime air over the Cordillera de la Costa (Rutllant et al. 2003; Muñoz et al. 2011). Along coastal cliff of the Atacama (a steep natural wall standing up to about 1000 m a. s. l.), the cloud can take the form of orographic fog (Cereceda et al. 2002). More extensively, the advective fog mantle typically appears along coastal areas between 700 and 1000 m a. s. l. over the Cordillera de la Costa. Inland fog is rare and is usually referred to occur as radiation fog during dawn (Cereceda et al. 2002; Schween et al. 2020). Ocean moisture and fog is advected inland more frequently through topographic depressions and corridors that bring maritime conditions far to the east where inland hyperarid conditions dominate (e.g., between about 1000 and 2500 m a. s. l.) (Farías et al. 2005; Cereceda et al. 2008b). The latter has important effects for distribution and persistence of airplant *Tillandsia landbeckii* (Pinto et al. 2006; Latorre et al. 2011; Koch et al. 2019) (Fig. 1).

Tillandsia landbeckii forms distinct vegetational patches, known locally as "tilandsiales," between about 900 and 1300 m a. s. l. on the Cordillera de la Costa, about 10–15 km away from the coastline (Pinto et al. 2006; Koch et al. 2020; Fig. 1). It is a widely accepted idea that this rootless plant obtains most of its water and nutrients from fog, and thus has been proposed as an indicator for paleo fog variability (Latorre et al. 2011; Jaeschke et al. 2019). The tilandsiales thus often are thought to reveal the highest elevation reached by fog on a regular basis and therefore mark the inland/upper limit of the Atacama fog Desert (Weischet 1975; Cereceda et al. 2008a). The *Tillandsia landbeckii* grows on sand dunes and forms a distinct banded pattern that can extend over a continuous surface for several km (Borthagaray et al. 2010). Such *Tillandsia* "stripes" tend to form perpendicular to the frequent daytime SW winds. At present, these desert ecosystems have been shown to occur in their present form since several millennia and are likely well adapted to the fog annual cycle and its interannual variability (Latorre et al. 2011; del Río et al. 2018; Jaeschke et al. 2019).

Fog along the coastal northern Chile is the main source of water for such ecosystems. It influences the chemistry of the soil and the formation of soluble salts in the soil (Voigt et al. 2020), provides water to several fog oases along the coastal cliff including life forms from biocrusts to higher plants like cacti and xerophytic shrubs (Muñoz et al. 2011) and last but not least provides water and nutrients to the highly specialized *Tillandsia landbeckii* (González et al. 2011; Koch et al. 2019). Here, we use observations at different elevations along the Cordillera de la Costa at the Estación Atacama UC Alto Patache and above the airport of Iquique in Cerro Oyarbide to characterize the climatology of the Atacama fog Desert. We use this opportunity to discuss detailed climate conditions affecting the *Tillandsia* ecosystems along the coastal–inland desert boundary. It has been shown that the maritime stratocumulus undergoes seasonal variations with elevated cloud bases and lowest occurrences in summer, and the lowest elevations and highest occurrences in winter (del Río et al. 2021a). Beside of this, a long-term decrease in cloud base height has been observed (Muñoz et al. 2016). It is unclear how this influences the occurrence of fog and Tillandsia geographic distribution in northern Chile.

Materials and methods

We selected the Cerro Oyarbide (OYA) and the Alto Patache (AP) fog oases where multiple meteorologic stations have been installed. OYA site is located above Iquique airport on the Cordillera de la Costa, as far as 11 km from the coastline (Fig. 1). Here, *Tillandsia landbeckii* fields develop on an undulated topography between 900 and 1300 m a. s. l. (Pinto et al. 2006; Mikulane et al. submitted to this Issue). AP site is just above the coastal cliff, on the westernmost margin of the Cordillera de la Costa, three km from the coastline. Maximum elevation here is 850 m a. s. l., at the southernmost point of a N–S topographic ridge. In this paper, we discuss data from OYA1211 and OYA780 stations in Cerro Oyarbide, and from AP850 and AP750 stations in Alto Patache (Fig. 1, Table 1). The names of the stations indicate their location (OYA, AP) and their respective elevation (1211, 850, 780 and 750 m a. s. l.). Whereas OYA1211 was installed at the top of a *Tillandsia landbeckii* field, thus aiming to characterize the direct atmospheric conditions at this place, OYA780 is located at a lower elevation 6 km to the SW. Both stations occur at a similar distance from the coastline (near 11 km) and from the coastal cliff (near 6 km) (Fig. 1). Both AP stations are close to each other at the costal cliff top in the Estación Atacama UC Alto Patache, separated by about 100 m elevation and 0.9 km horizontal distance. They occur 2.5 km from the coastline. 40 km and 30 km separate OYA1211 and OYA780 from AP stations, respectively. In addition, the meteorological station located at Iquique Airport (20° 32′ 28″ S–70° 10′ 38″ W) in the coastal plane at 56 m a. s. l. has been included as a surface reference to analyze data in the entire MBL. In summary, the network of four stations spans from the eastern main heights to the westernmost margin of the coastal mountain relief (Fig. 1). Therefore, the collected data from these meteorological stations reveal the temporal and spatial variability of the low-level atmosphere over the Cordillera de la Costa. Previous studies have included annual meteorological data from some of these stations (Cereceda et al. 2008b; Lobos et al. 2018; Schween et al. 2020).

Meteorological data discussed in this paper include: temperature (T), relative humidity (RH), wind speed (WS), wind direction (WD), air pressure (AP) fog presence (FP) and fog water (FW) (Table 1). For analyzing the

Table 1 Meteorological stations and measured variables

Meteorological station name	Lat/Lon	Elevation (m a. s. l.)	Distance to coastline (km)	SFC azimuth	Atmospheric variable	Instrument	Data logger
OYA1211	20° 29′ 28″ S/70° 03′ 31″ W	1211	11.4	245	T	Hygro-Thermo Compact Thies	Thies DL16
					RH	Hygro-Thermo Compact Thies	
					FW	SFC + pluviometer	
					FP	Thies 5.4032.35.007	
					WD	Wind Dir. Compact Thies	
					WS	Wind T. Compact Thies	
OYA780	20° 31′ 59″ S/70° 05′ 35″ W	780	11.1	250	T	Hygro-Thermo Compact Thies	Thies DL16
					RH	Hygro-Thermo Compact Thies	
					FW	SFC + pluviometer	
					FP	Thies 5.4032.35.007	
					WD	Wind Dir. Compact Thies	
					WS	Wind T. Compact Thies	
AP850	20° 49′ 35″ S/70° 08′ 53″ W	850	3.85	190	T	WXT530	CR1000
					RH	WXT530	
					FW	SFC + pluviometer	
					FP	Young/52203	
					WD	WXT530	
					WS	WXT530	
AP750	20° 49′ 32″ S/70° 09′ 23″ W	750	3	180	T	Campbell/HC2S3	CR1000X
					RH	Campbell/HC2S3	
					FW	SFC + pluviometer	
					FP	Young/52203	
					WD	Young/01503	
					WS	Young/01503	

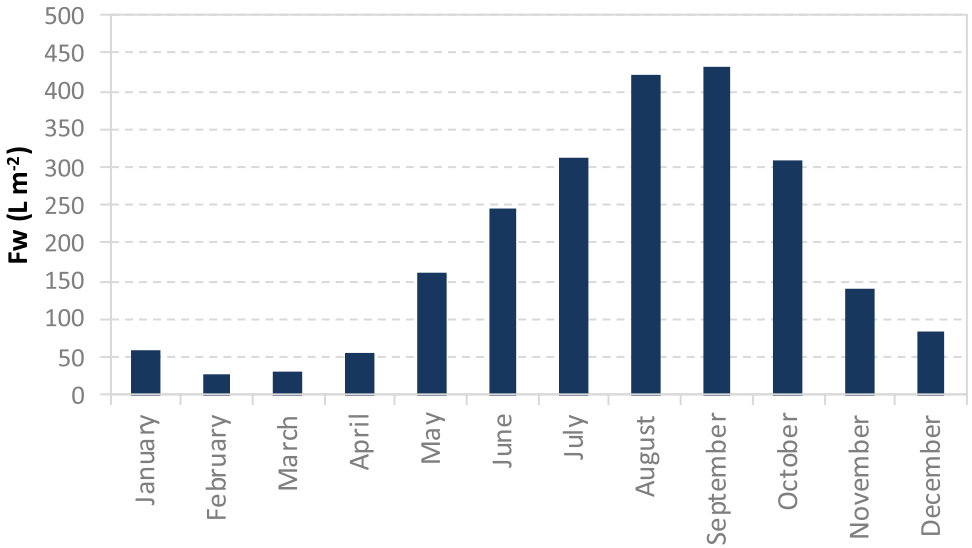

Fig. 2 Mean fog annual cycle as seen from Alto Patache fog water (Fw) collection in AP850 (1998–2013). Note that July, August and September (JAS) are the three main months

inland advection of marine air masses, we characterize the potential temperature (θ) and specific humidity (q) vertical gradients between the meteorological stations close to the sea level and up in the Cordillera de la Costa highlands. These gradients allow us to quantify the presence of the well-mixed marine boundary layer in a site that is related to advective fog. The fog variables are measured by a one-square meter standard fog collector (SFC) (Schemenauer

Table 2 Data availability from stations used in this paper

	AP850 (%)	AP750 (%)	OYA1211 (%)	OYA780 (%)
July 2018	100	100	100	92
August 2018	100	100	100	100
September 2018	100	100	97	12
JAS 2018	100	100	99	69
July 2019	100	100	100	100
August 2019	100	100	100	82
September 2019	100	100	100	100
JAS 2019	100	100	100	94

% values indicate data available for the studied period (JAS 2018 and JAS 2019). Values describe the data availability for all meteorological variables, with three exceptions: *Sep_18_AP750*: 9% of the RH data are available; *Aug_19_OYA780*: 100% of the WD and WS data are available; and *Sep_19_OYA780*: 96% of WD data are available

and Cereceda 1994) connected to a pluviometer. It measures the water collected by the upright standing SFC given in L m^{-2}, i.e., the amount of water collected by surface area of the collector. Despite the different geometry and surface properties compared to plants, we interpret this as a measure for the water amount a plant may collect from fog. We use data from the 2018 and 2019 July–August–September months (the JAS period) because they represent the peak of the fog season at 20° S (Cereceda et al. 2008a; Muñoz et al. 2011) (Fig. 2; Table 2). At this time of the year, the fog deck reaches the upper Cordillera de la Costa tillandsia fields more frequently than during summer when a fogless season occurs (Cereceda et al. 2008b). We show results based on one-hour averages of the data. In some cases, we use 10-min data to denote extreme variability and detailed fog event characterization. We first converted the data to local time (UTC-4). Then obtained the hourly means based on the 10-min data. For wind direction, we obtained a vectorial hourly mean. FW data were calculated as the accumulated total per hour expressed as l m^{-2} h^{-1}. To make our FW data comparable, we also include a daily mean l m^{-2} d^{-1}.

Whereas FW values for OYA stations are directly transformed from the data logger reading in ml to L m^{-2}, for AP stations L m^{-2} were obtained after applying the following formulae:

Fog water for AP (FW_AP) is calculated from the pluviometer readings (N in mm) as follows:

$$\mathrm{FW} = \frac{N}{N_0} \cdot v_{\mathrm{cup}} \tag{1}$$

with $N_0 = 0.1$ mm the basic pluviometer reading per cup flip over and v_{cup} is the cup volume in liter of the different pluviometers (5E−3 l and 2.25E−3 l for AP805 and AP750, respectively). According to the Young 52,202 manual, the volume of the bucket is 2 ml, but we use 2.25 ml as we tested in the field several times.

FP is directly inferred from the FW data as times where FW > 0.

$$\mathrm{FP} = \begin{cases} \text{true} & : \mathrm{FW} > 0\ \mathrm{L/m^2} \\ \text{false} & : \mathrm{FW} = 0\ \mathrm{L/m^2} \end{cases} \tag{2}$$

We are aware that a SFC needs some time to be sufficient wetted for the fog water to flow into the pluviometer and that it also needs some time to dry after fog has ended. But these delay times are usually small compared to fog duration. The FP statistic should be regarded as an underestimation of the real fog presence value, which may be larger as fog presence does not necessarily produce fog water collection. Nonetheless, from other observations we know that variable FW > 0 is a very good indicator for the presence of fog (del Río et al. 2018).

Fog data are recorded when fog comes from within the anterior and posterior 90° angle range. We are certain that SFCs will mostly fail to record fog advected exactly from the sides (e.g., parallel to the SFC panel), but at any oblique angle the panel should intersect fog and record data, thus evidencing fog presence (i.e., a fog event). This is expected as wind is always veering around the average direction, even under stable calm conditions. Therefore, we expect that wind from the side of the collectors occurs only occasionally but should be regarded with caution. Wind direction may influence collection efficiency, but we are not aware of a correction for this. It is assumed that fog trespassing the SFC mesh at right angles will record more fog water than oblique approaching fog, but in both cases a fog event is recorded. We are aware that in some cases, we may be missing fog events (see also discussion section).

In order to characterize fog variability, we also carried out a detailed fog event analysis. We defined a single fog event when the SFC records FW for 60 min or more. FW collection can occur at intermittent time lapses within a fog event but if FW occurs separated by more than 60 min it is considered to be part of a different fog event. Fog events were named by the principal wind direction that characterize the event (e.g., NE or SW) when at least during 80% of the time wind remained in the associated 90° quadrant. When the principal wind quadrant occurred less than 80%, the event is called a "composite fog event." For instance, the fog event "NE" includes the 90° quadrant: N, NE and E, all of them together adding ≥ 80% within this fog event. If they add < 80%, implying that rather other wind directions occur through the fog event, we named this composite

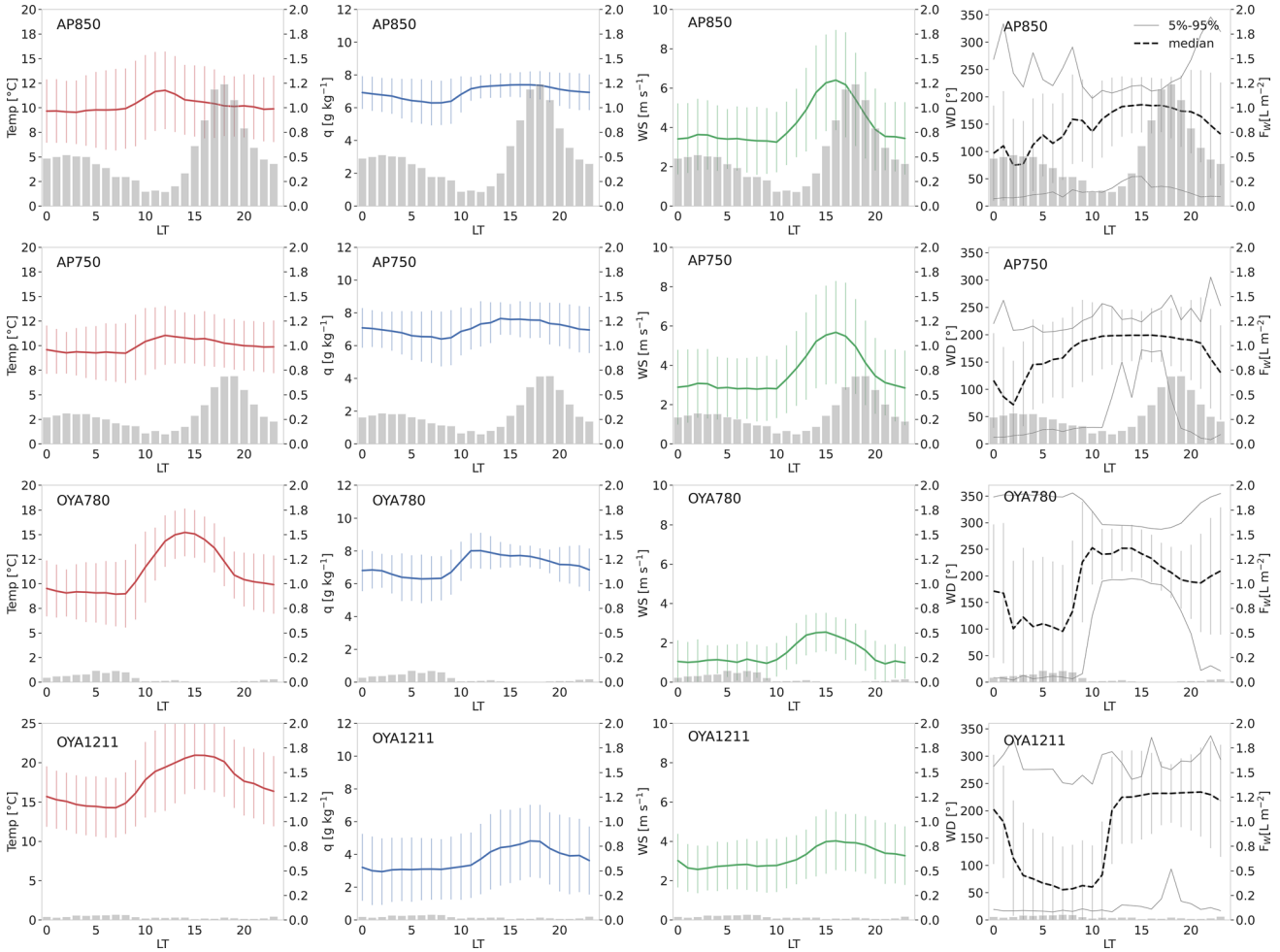

Fig. 3 Meteorological conditions during the JAS period. Air temperature (1st column), specific humidity (2nd column), wind speed (3rd column) and wind direction (4th column) contrast with fog water (right Y axis in bars). Fog water means include all data (fog and no fog data so include a representative scenario). Error bars indicates the one standard deviation of meteorological variables. In the 2nd column, note the steep increase of q first in the lower and then in the upper stations, in all cases indicating the advection of moisture from the coast inland though the day when ocean–continent winds dominate. In the 4th column, dashed line is the median (percentile 50%) and light gray lines the 5 and 95% percentiles

fog event accordingly (e.g., "SW–NE" fog event, that result from S, SW, W and N, NE and E wind directions altogether adding ≥ 80%). The order of the wind components does not imply wind directions veering, only the wind quadrant components. We did not consider for our analysis events that do not agree with this criterion (i.e., fog event events with extreme WD variability), which, in any case, are uncommon. Each fog event this way defined was described also in terms of their start and end time, mean duration and FW yield.

Results

In this section, we describe the main aspects of the meteorological and fog data from the Alto Patache and Cerro Oyarbide sites.

Temperatures

The mean T reach their minimum (min) during early morning (06–08 h.) and maximum (max) at noon (AP) and afternoon (OYA.) (see Fig. 3). Whereas mean min in OYA varied from 9.0 °C (OYA780) to 14.5 °C (OYA1211), in AP it varied from 9.3 °C (AP750) to 9.6 °C (AP850). Similarly, mean max in OYA varied from 15.0 °C (OYA780) to 21.0 °C (OYA1211); in AP, it varied from 10.9 °C (AP750) to 11.3 °C (AP850). In both sites, the higher mean T occur at higher elevations (Fig. 3). The daily mean air temperature amplitude in AP is < 2 °C at both AP stations, whereas in OYA it reaches 6.0 °C in both stations. Despite the similar elevation and nearness of OYA780 and AP750 stations, the OYA780 mean T is 11.1 °C, but in AP750 °C is 10.0 °C (same mean as in AP850). Moreover, the mean

daily oscillation is > 4 °C larger in OYA780 compared to AP750. Yet OYA780 air temperatures are closer to AP750 and AP850 than to those higher in elevation in OYA1211. The OYA1211 mean temperature of 17.3 °C is significantly higher (6 °C) than that at OYA780. Absolute max and min in OYA1211 reached 30.2 °C and 2.3 °C, respectively. OYA1211 site presents the most extreme absolute air temperature difference (25 °C) recorded during the afternoon (in different days). The other three stations recorded a smaller delta absolute temperature, but, in all cases, a wide temperature range occurs.

Humidity

Relative humidity is mostly above 80% in AP, more humid than in OYA780. In contrast, hereto OYA1211 experiences values close to 30% RH. AP and OYA780 stations show a gradual RH decrease through the night, which is opposite to the higher located OYA1211 (not shown). Also, whereas the min occurs during afternoon in OYA780, it occurs during the morning in the three other AP and OYA stations. Extreme RH values were recorded in all stations, with OYA1211 covering the whole RH range (minimum of 0.8%). In summary, mean RH values are high for both AP sites and OYA780, but low for OYA1211.

Because RH varies strongly with temperature, we calculate specific humidity (q) to detect the presence of maritime humid air (q high) or inland dry air (q low). Mean hourly q values at AP vary between 6 and 8 g kg^{-1} during a JAS day (Fig. 3). Both AP750 and AP850 parallel each other during the day–night cycle with slightly higher values reached at AP750. Min values occur during the early morning and max during late afternoon and nighttime. At OYA780, similar mean q values as at AP are recorded and similar daily cycle is observed, although a more marked daily cycle is observed. Much lower mean daily q occurs at OYA1211, ranging from 3 to 5 g kg^{-1}. Here, the day–night cycle shows a min during night and a max during late afternoon. Similarities and differences apply among stations regarding the q daily cycle. For instance, the AP and OYA780 stations show the diurnal behavior. However, the amplitude seen in OYA780 is larger (about 2 g kg^{-1}) than the one present at the AP stations (about 1.0 g kg^{-1}). At OYA1211, the q increase lags the other stations, starting gradually from 12 h. and reaching a peak at 18 h. This lag evidences the diurnal dynamic of moisture along the vertical elevation gradient, which naturally reaches the lower areas first and the upper ones later in the day.

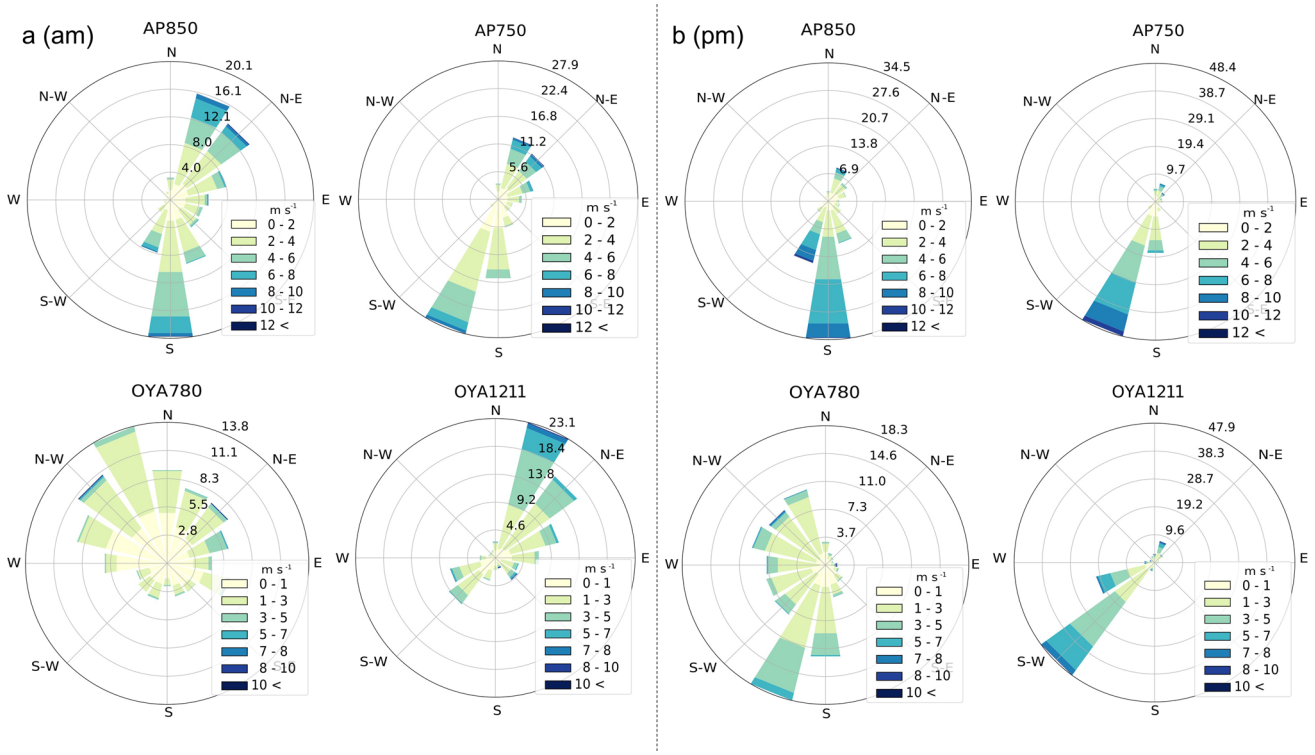

Fig. 4 Wind directions and speeds for the JAS 2018–2019 period at Cerro Oyarbide and Alto Patache. **a** am hours; **b** pm hours. All studied data are shown. Relative frequency for each wind direction is shown also (in %)

Wind direction and speed

Overall, the WD follows a day and night cycle at both OYA and AP sites (Figs. 3, 4). In particular, wind directions tend to be different between am and pm hours. In OYA, winds from the N–NW (OYA780) and N–NE (OYA1211) predominate during night, but from the S, SSW (OYA780) and SW (OYA1211) during the afternoon (Fig. 4). Wind directions at OYA show a clear and fast switch between easterly directions in the second half of the night and SW directions during daytime from morning till late afternoon. But nighttime directions vary strongly at OYA780. In AP, both stations parallel each other in terms of wind direction dynamic through day and night. Whereas daytime (pm) wind is dominated by the S (180°) component, nighttime (am) wind occurs either from the NE or S.

Wind speed commonly occurs between 1 and 6 m s^{-1} in the study area with AP comprising more intense winds compared to OYA stations. In both sites, winds are gentler during nighttime and more intense through the day. In OYA1211, highest persistent SW wind velocities occur during late afternoon with a median of 3.8 m s^{-1} and max of 10 m s^{-1}. In OYA780, a peak occurs during the early afternoon but mean is only 2.8 m s^{-1} and absolute maximum 9.9 m s^{-1}, therefore weaker and less persistent winds compared to OYA1211. Nighttime winds are normally around 2.6 m s^{-1} in OYA1211 and 1.5 m s^{-1} in OYA780. In AP, again the highest and more persistent winds occur in the afternoon, particularly between 14 and 18 h., when S to SSW winds normally reach 5 m s^{-1} in AP750 and 6 m s^{-1} in AP850. Maximum speeds were recorded also at this time frame reaching 12.9 m s^{-1} in AP850 and 12.1 m s^{-1} in AP750. Calmer wind during nighttime results in a mean close to 2.5 m s^{-1} in AP750 and 3.2 m s^{-1} in AP850.

Fog presence

There is a striking difference in terms of fog presence (FP) between AP and OYA (Fig. 5). Fog in AP occurred 73% of the time during JAS 2018–2019, which contrasts with the 76% of fog absence in OYA in the same period. In OYA, fog occurred mostly at OYA780 (19% of the JAS) and only during very limited time in OYA1211 (6% of the JAS). Only 1% of the time both OYA1211 and OYA780 experienced simultaneous fog. In AP, fog occurring simultaneously at both AP750 and AP850 is the most common case (49%). This is expected as both stations occur close to each other (i.e., separated by 100 m elevation and < 1 km distance). Available data indicate that fog at AP750 is more frequent than at AP850: AP850 is fog-free during 44% compared to 34% of the JAS time for AP750.

If one considers now the diurnal course of fog presence, similarities and differences are observed among stations. Overall, low relative FP frequency occurs from noon to evening and high FP during night and morning in all stations (Table 4). Nonetheless, the afternoon fog gap in OYA stations is prominent compared to AP. In AP, a more regular FP frequency distribution occurs through day and night and only tends to dissipate during midday. This is more obvious at AP850 compared to AP750, the latter experiencing more frequency of FP. At the AP site, the daily cycle starts from a minimum when 5% (AP750) and 10% (AP850) of the daily FP is recorded during the early afternoon (12–15 h.). Then it gradually increases to reach a long period with higher FP frequency from evening through the night until morning

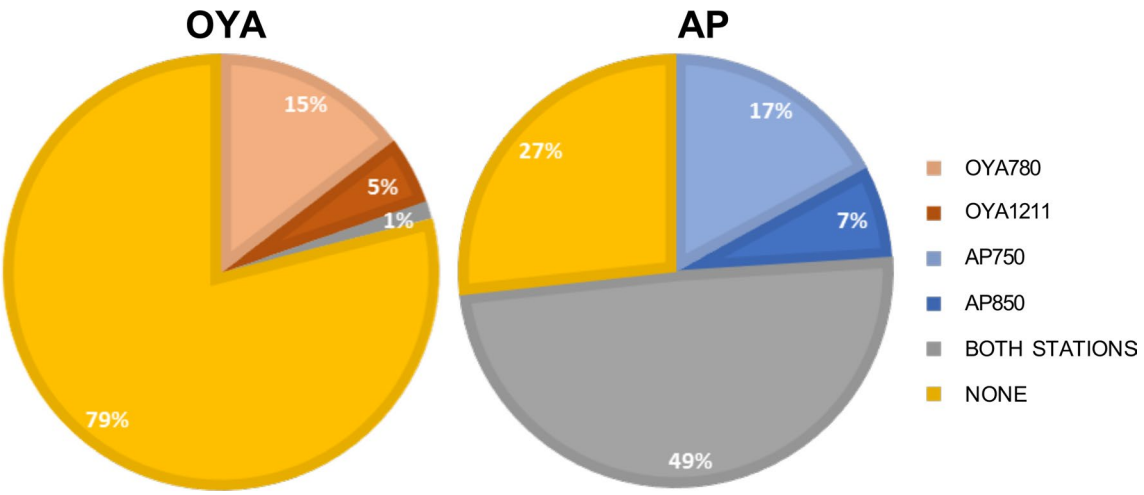

Fig. 5 Fog presence (FP) and its distribution at the stations in Cerro Oyarbide (OYA) and Alto Patache (AP) sites. Percentages are relative to total of JAS periods in 2018 and 2019 at each respective site. "BOTH" in gray color means that at each site both stations record FP simultaneously; opposite, "NONE" means no FP is recorded in AP or OYA

Table 3 Fog water collection (L m^{-2}) at all four stations in OYA and AP

	AP850	AP750	OYA1211	OYA780
July 2018	361	301	25	38
August 2018	460	279	6	25
September 2018	337	168	11	1
JAS 2018	1158	748	42	64
July 2019	428	243	39	44
August 2019	298	145	8	15
September 2019	400	208	31	14
JAS 2019	1126	596	78	73
Total (L m^{-2})	2284	1344	120	137
(L m^{-2} day^{-1})	12.4	7.3	0.7	0.9

Please see Table 2 for information about data availability. For instance, during September 2018 OYA780 includes only 12% of the data, thus representing a minimum value

when fog starts to dissipate. While OYA1211 follows an overall similar trend as in AP, OYA780 is different. Here, FP increases trough night until early morning. Moreover, the night–morning FP trend in OYA780 is out of phase compared to AP stations. Virtually no fog occurs from noon until evening for the studied period in OYA780 but occasionally the fog cloud occurs in OYA1211 at this time of the day. 96% of FP occurs during nighttime and morning in OYA780 (mostly at dawn), and 82% occurs in OYA1211 at the same time.

Fog water

Fog presence and fog water data are obtained from the fog water collection record and both variables follow similar day–night trends. In AP, most fog water is collected between 16 and 20 h. and a second max at 01–04 h. (Fig. 3; Table 4). During late afternoon time, about 45% of the total daily fog water is collected in both AP stations (Fig. 3). During nighttime, near 35% of fog water is collected in AP. On the other hand, OYA stations collect most its fog water through night and mostly early morning (80% in OYA780 and 55% in OYA1211 between about 00 and 08 h., Fig. 3; Table 4). Afternoon fog collection in OYA780 is very rare but more common in OYA1211.

Monthly FW volumes are up to two orders of magnitude larger at AP than at OYA stations (Table 3). Whereas the JAS period mean in AP850 can surpass 1000 L m^{-2}, at OYA (both stations), yields are below 80 L m^{-2}. Both stations in OYA collect a similar amount of fog water despite the difference in elevation. Nonetheless, the volumes from OYA780 in September 2018 are only minimum values (see Table 2). In contrast hereto, AP850 fog water yields are between 1.5 and 2.0 times those recorded in AP750 (672 L m^{-2} vs. 1142 L m^{-2}), despite the fact that both stations are relatively close to each other and that FP is greater at AP750. The max monthly FW yield was collected in AP850 August 2018 reaching 460 L m^{-2}, which is in strong contrast to the max of 44 L m^{-2} recorded in OYA780 in July 2019. On a mean daily basis (considering only the days with available data), OYA780 collected 0.9 L m^{-2} day^{-1} and OYA1211 collected 0.7 L m^{-2} day^{-1} during the studied period. AP750 collected 7.3 L m^{-2} day^{-1} and AP850 12.4 L m^{-2} day^{-1} for the studied period. For the periods JAS 2018 and JAS 2019, total fog water yields do not change much at each station, which could indicate certain regularity in the system across the years. In fact, the FW values reported here are comparable with those reported by Cereceda et al. (2008b) for this time of the year in Alto Patache and in Cerro Guatalaya, which is located at a similar elevation and distance to the coast as OYA1211, but few tens of km to the north.

Discussion

Wind

We know about two distinct wind systems in the area: the southeast Pacific high-pressure system (SEPH) that drives the coastal low-level jet, i.e., a nearly permanent strong southerly wind component in the maritime boundary layer (MBL) below about 1 km (see, e.g., Muñoz and Garreaud 2005). This can clearly be seen at the three lower stations, particularly in AP site. In OYA1211, only afternoon SW winds are recorded (Fig. 4b). Superimposed over the southerly flow of the SEPH, a land–sea breeze develops in the MBL at the coast and may lead in the upper half of the MBL to southeasterly flows during daytime and southwesterly flows during night. This should be stronger if a coastal plane is present, as it occurs south of Iquique, which allows significant surface heating. Nevertheless, this is not visible in the presented mean data.

At heights above the MBL and especially further inland the so called Rutllant cell (Rutllant et al. 2003), initiated by radiative heating and cooling at the slopes of the Andes and the Altiplano to the west leads to strong westerly and easterly winds during daytime and nighttime, respectively (Schween et al. 2020). During daytime (nighttime) the air ascents (descends) along the western slope of the Andes, flows around 3–4 km upwards (downwards) back to the west and subsides (rises) above the central depression and coastal mountains of the desert. We observe the wind components as NE and SW during night and afternoon, respectively, particularly at the upper OYA1211 station which may indicate that the subsiding branch of the Rutllant cell reaches the coast and may extent over the ocean. The variable wind directions and reduced wind speeds at OYA780, 11 km from the coastline, could be an indication of afternoon (night)

subsiding (rising) at this location. In any case, the discussed circulation pattern represents idealizations that are subject to modification by the local orography, which may channel and redirect the flow, and in addition may lead to the development of local thermal circulations. Overall, the OYA terrain is sloping from NE down to SW (i.e., toward the ocean). During night, a density-driven flow would follow this slope and generate NE wind. During daytime, solar heating would lead to upslope flow with SW directions. Both directions are visible at OYA1211, whereas at OYA780 only the daytime SW flow seems to be present. At AP, the topography is different. Both stations lie directly at the top of the coastal cliff, which runs here for about 1 km from W to E facing south. During daytime, the dominating S wind indicates the southerly wind of the SEPH, probably enhanced by a sea breeze. During the night, two regimes can be observed: During the first half of the night, S wind further dominates but during the second half of the night wind switches to E to NE wind indicating influence of the nighttime flow of the Rutllant cell.

Temperature and humidity

The T and q variability can be extreme in space and time within the coastal Atacama (Lobos et al. 2018; Schween et al. 2020). Air temperature extremes increase inland, as expected, reaching as low as 3 °C and up to 30 °C, with a mean of 17 °C, at OYA1211 in JAS. The milder temperature and its limited daily variability at AP750 (9–11 °C) can be explained by its location directly at the cliff (i.e., most of the time inside the MBL), where the temperature is regulated by the ocean. OYA780 is inland and measures conditions of the land–surface boundary layer, i.e., is influenced by surface heating with larger daily amplitudes. At OYA1211, we observe very low q values that mostly lie below 4 g kg^{-1} with RH most of the time below 40% and as low as 1% RH. This is in contrast to the lower stations (OYA780, AP750 and AP850) where low temperatures (mean close to 10–11 °C) and humid air (mostly > 5 g kg^{-1} and > 80%) indicate that these stations are more frequently in the moister and cooler MBL (Rutllant et al. 2003; Muñoz et al. 2011; Schween et al. 2020). Extremes spatial gradients occur also. For instance, we observe that OYA780 can be at 6 g kg^{-1} and 11.5 °C, but OYA1211 2 g kg^{-1} and 28 °C at the same time. Such opposite conditions between the stations can be attributed to the large differences between the MBL extent and the free troposphere above, which can reach temperature and humidity differences of more than 10 °C and 5–6 g kg^{-1}, respectively (Muñoz et al 2011). Also notable, we record station-specific rapid changes. For instance, shifts of 4 °C, 50% HR and 5.5 g/kg in 10–20 min occur in OYA780 and AP850; or changes of 7 °C, 60% and 2.5 g/kg within 10 min in OYA1211. The observed behavior could be then linked to air masses advection across the coastal area associated, or not, with the altitudinal change of the MBL top. We discuss this further in the next paragraph. In any case, the data clearly show the rapid exchange between the upper inland desert atmosphere and the lower marine atmosphere.

At OYA1211, the mean daily cycle shows that the T and RH (the latter not shown in Fig. 3) gradually increase together after a late morning minimum (9–12 h.). With sunset, T declines but RH does not. In fact, a positive RH trend is also recorded during nighttime in OYA1211, when in all other stations in OYA and AP show an overall decreasing RH trend. Therefore, the mean RH is rather out of phase between upper and lower stations during nighttime. The RH min in OYA1211 and AP stations occurs before the afternoon peak in T, but in OYA780 coincides with this afternoon peak, when OYA1211 RH is already increasing along with air temperature. The data suggest that air temperature alone cannot explain the observed RH changes. Consistent to RH, the Fig. 3 shows an increase of q during morning and later in the afternoon in the AP-OYA780 and OYA1211 stations, respectively, and therefore the advection of moist maritime air inland through the day at least as high as 1211 m a. s. l. Opposite, the mean decreases of q during nighttime in AP and OYA implies inland desert air replacing the maritime air at these locations. One potential way to explain these observed changes in moisture content is through the daily elevation changes of the MBL that distribute marine air through the coastal desert as high as about 1300 m a. s. l. Nonetheless, as far as predicted by the Rutllant pump circulation model, the MBL reaches its lowest (highest) elevation during day (night), which therefore cannot explain the observed moisture changes at AP and OYA stations. The model suggests daytime enhanced coastal air subsidence above the temperature inversion on top of the MBL that promotes cloud dissipation and mostly unlimited ceilings that best describe inland desert influence at least as low as the AP site (Rutllant et al. 1998, 2003; Muñoz et al. 2011). High potential temperature (θ) gradients between the airport and OYA1211 confirm a mean afternoon stratified condition including Cerro Oyarbide (see Fig. 6c, d). Opposite, lower θ gradients suggest a better mixed layer at 1211 m a. s. l. occurring during night, much later than the observed increase in local moisture. Alternatively, the observed moist trends can be explained by a "mountain vent system," which suggest that along the slopes of the coastal cliff and higher slopes of the cordillera (e.g., Cerro Oyarbide) air is heated and flowing in a thin layer (d ~ 50 m) along the surface upward bringing moist air from the MBL during daytime. To decide which of the two mechanisms lead (higher MBL or mountain vent/slope wind) to the presence of maritime air at the upper stations, it would be necessary to investigate temperature profiles away from the surface. The implication is that afternoon vigorous SW winds (ocean–continent) carry

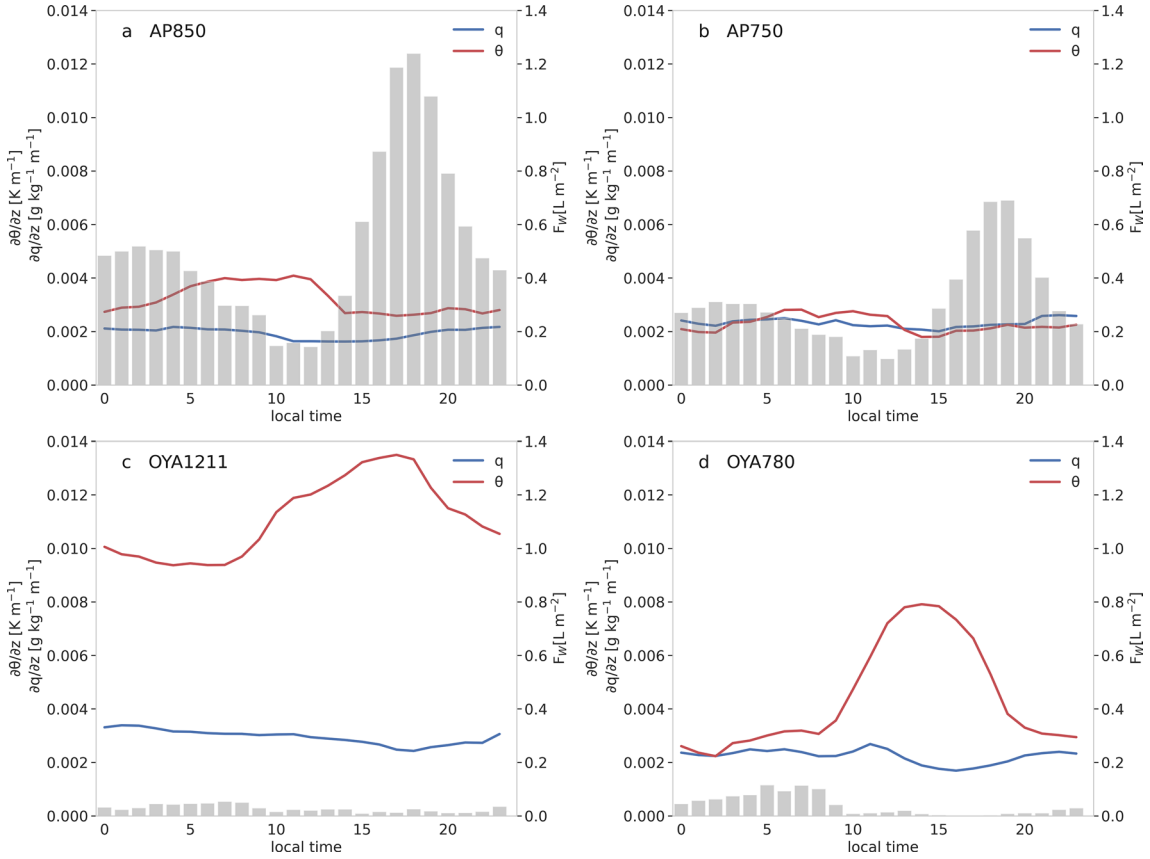

Fig. 6 Potential temperature (θ) and specific humidity (q) gradients between airport station and **a** AP850, **b** AP750, **c** OYA1211 and **d** OYA780 meteorological stations. Fog water is represented in gray bars. In general terms, the gradients show the relation between fog formation and dissipation, presenting low values when fog is present and high ones when fog is absent. This is well shown by the θ data and to a less degree by the q data. A stronger θ daily cycle in OYA sites implies that are more commonly dominated by desert air masses than AP stations

maritime moist air upwards producing a significant increase in local humidity inland at least as high as 1211 m a. s. l. Reversed night winds (continent–ocean) bring dry continental air to the coast dropping moisture values at 1211 m a. s. l. and below (Fig. 3).

Fog formation and dissipation

The MBL can include two atmospheric regimes: (1) the well-mixed regime, associated with fog formation, low thermal and humidity vertical gradients, low diurnal variability and presence of Sc cloud fog; and (2) the stratified regime related to warm and dry continental air masses and high thermal and humidity gradients associated with fog dissipation (Lobos et al. 2018). The atmospheric regimes studied by Lobos et al. (2018) set a threshold from where fog is formed or dissipated. This threshold is based on the thermal and moisture gradient over a vertical section of the MBL. The proposed thresholds under which fog would form are 0.0031 K m^{-1} and 0.0016 g kg^{-1} m^{-1} (the horizontal line in Fig. 7). We statistically analyze the vertical gradients between the airport station and each meteorological station in the transect, during fog and non-fog over the JAS (Fig. 7). On the one hand, gradients during fog presence are lower compared to fog absence. The low gradients denote a strong mixing within the MBL, which has been demonstrated as a fundamental condition for fog formation (see Lobos et al. 2018; Duynkerke et al. 1995). Opposite, high gradients denote a stratified regime linkable to fog absence. However, the gradient medians do not change significantly between fog and non-fog conditions in AP and OYA780 stations, the opposite being true at OYA1211, thus denoting the dominance of marine air toward lower elevations compared to higher elevations and thus showing the need for MBL air to be present at higher altitudes in order for fog to exist there. Thus, differences between AP and OYA stations, regarding the vertical gradients during fog and non-fog conditions, are given by the predominance of the MBL over the stations. Our data show that during JAS, thresholds set by Lobos et al.

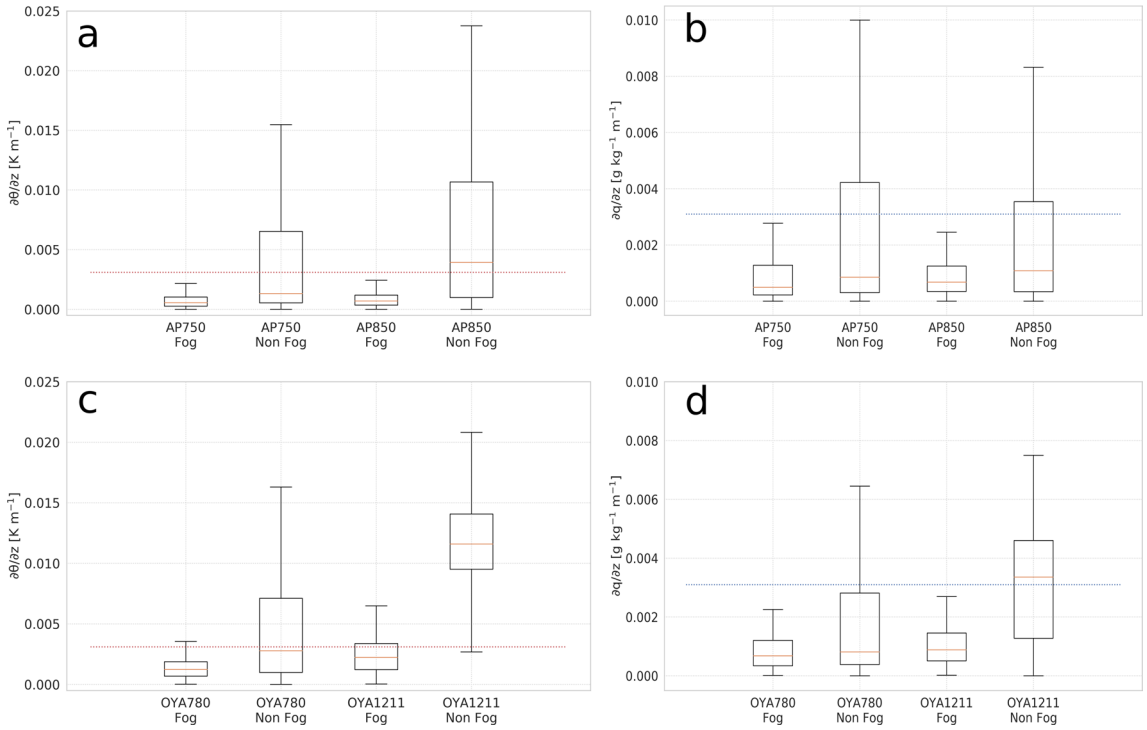

Fig. 7 Descriptive statistics of thermal (**a**, **c**) and moisture (**b**, **d**) vertical gradients between the airport meteorological station and AP750, AP850, OYA780 and OYA1211 stations. The horizontal line represents the threshold value established by Lobos et al. (2018) to differentiate fog formation and dissipation

(2018) are overestimated and can be improved to be more accurate in predicting fog formation.

From the above paragraph, we observe that the vertical mixing and the stratified atmospheric regimes in the Coastal Atacama boundary layer are associated with fog formation (presence) and dissipation (absence), respectively. During midday, fog absence/low fog collection in AP (Fig. 5a, b), the gradient θ is higher and variable, implying that at this time both stations, or at least the upper AP850, occur within the stratified regime above the well-mixed MBL (morning–early afternoon); opposite, when fog is present, the gradient θ is lower than 0.0031 K m^{-1}, as expected when both stations occur within a well-mixed MBL and fog water collection reaches a maximum (afternoon through night). The same trends that we find for AP occurs in OYA. For instance, mean air temperature can be up to 6–8 °C higher in OYA1211 compared to OYA780 during fog absence denoting stratified conditions in this altitudinal range during the afternoon. However, when fog is formed, θ gradients are the lowest recorded suggesting a well-mixed marine air up to 1211 m a. s. l. during night–early morning (Fig. 5c, d). Altogether, the data suggest a diurnal cycle regarding the influence of the inland versus marine desert conditions throughout the coastal Atacama, which in turn denote a regional-scale atmospheric circulation.

Distinct atmospheric and fog conditions occur between OYA780 and AP750 despite their similar elevations and geographic proximity. Despite similar daily *q* evolutions of both stations (increasing during morning, Fig. 3), the *θ* gradients at OYA780 show a more marked diurnal cycle compared to AP750 (Fig. 6b–d). Thus, q data indicate that both sites are under the effect of the advection of marine air at the same time, but the influence of inland dry air is conspicuous in OYA780 compared to AP750. In other words, in OYA780 the daily interchange between marine and continent air is more common in OYA780 than in AP750, which keeps a more uniform day-to-day marine condition. This is to be expected because OYA780 is 11 km away from the coastline and AP750 about 2 km away, on the coastal cliff. As a consequence, fog is much more common in AP. In fact, only 22% of fog presence at AP750 corresponds to fog at OYA780, but 95% of OYA780 FP corresponds to FP at AP750. In the former scenario, OYA780 experiences higher than normal RH (> 85%) showing enhanced maritime air characteristics, but no condensation into fog. When no fog occurs either at OYA780 or at AP750 simultaneously, the mean RH is low and the T increase significantly with respect to the mean at both sites, suggesting an MBL stratified regime at 750 m a. s. l. All together, these observations suggest that the MBL elevation fluctuates uniformly within the coastal Atacama

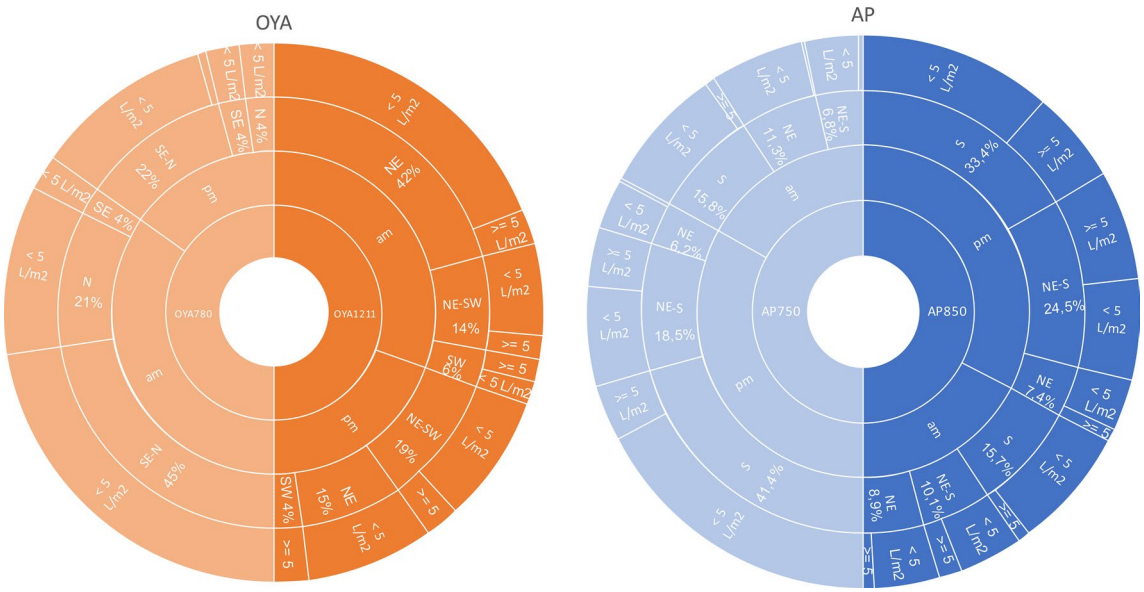

Fig. 8 Distribution of fog events types per stations (AP750, AP850, OYA780, OYA1211) per time of the day (a.m. and p.m.), wind direction (N, NE, S, etc., 90º quadrant) and fog water amount (collection per event below or above 5 L/m^2, described for the JAS 2018–2019 in Cerro Oyarbide (CO) and Alto Patache (AP)). The length of each sector gives the relative contribution (%) and associated water yield of each fog event type. Data are presented relative to total fog events recorded at each meteorological station (see text for more details). Some fog data may not be recorded by our data given the directional nature of the SFCs

and that both distance to the coastline and elevation above sea level are controlling factors to the observed dynamics.

Fog events

In this section, we discriminate the most representative fog events that occur at the coastal Atacama. We characterized fog events in detail including start–end time, duration, wind and fog water collection, which contribute to a better understanding of fog distribution, space and time (Fig. 8). Fog events are named after the predominating wind direction (please refer to the method section for details on how a fog event was defined).

Due to their construction SFC are not sensitive for fog when wind is blowing from the side. All SFC were installed such that they face the expected average wind direction at every location (see azimuth in Table 1). Figure 4 shows the wind roses from observed wind for all four stations. For both AP stations and OYA1211, winds from the side of the SFC make up between less than 10% (AP750 and OYA1211) and around 15% (AP850). At OYA780, wind directions are highly variable and the SFC may miss some fog events. Veering of the wind may still produce some fog water, and thus, the events will be counted although the amount of fog water might be underestimated. A cylindrical or bidirectional flat SFC design may fit better the local meteorological conditions at this station. Nevertheless, cylindrical fog collectors show lower efficiencies and a different wind speed dependence and are thus difficult to compare with the SFC (Regalado and Ritter 2016).

In Alto Patache, the S, S–NE and NE are the three most common fog events (Fig. 8); they sum up to 339 and 469 events in AP850 and AP750, respectively. The most common are the S events (50–60%) and the least common are the NE events (5–15%). Both of these are the shorter ones (mean duration 2–5 h) compared to the S–NE events (mean duration 8–11 h). Extreme and rare S–NE event durations can reach 33 h (AP850) and 98 h (AP750). The S–NE events embrace 50% of the total fog time in AP, which contrasts with the NE fog events that only adds < 10%. The remaining 40% of fog time is associated with S events. The S fog events are more common during the afternoon, the S–NE during the late afternoon onwards and the NE during nighttime (Fig. 8). Because of their long duration, the S–NE event includes a change in wind directions that follow the daily cycle (Fig. 4). A common case is a fog event starting with S winds during late afternoon and ending with NE winds during nighttime or dawn. The implication is that fog advection from the ocean–inland during the day (onshore) may reverse later during the same event with a near opposite wind direction (offshore). Longer events lasting until next day can start and end with S winds, and include NE in between. The NE events show a return fog flow toward the coast in response to concomitant predominant winds. Most fog water (up to 95%) is collected in similar proportions by S and S–NE events. Nonetheless, within a S–NE event, the

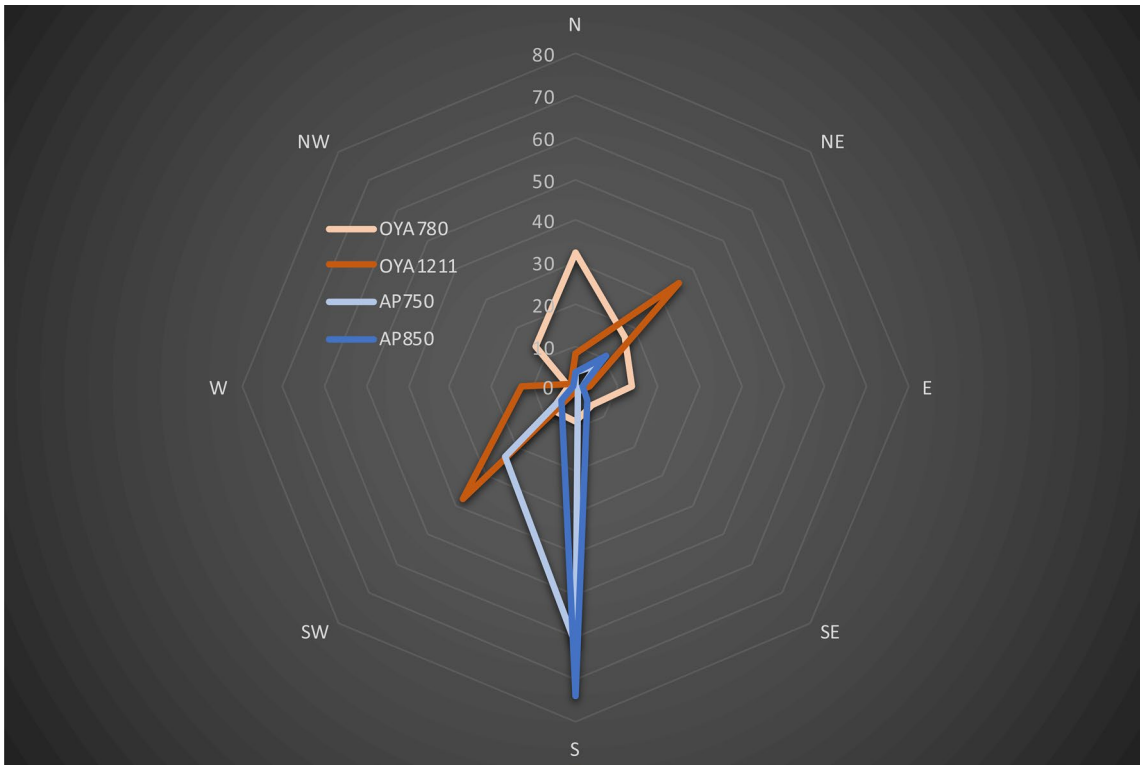

Fig. 9 Relative contribution (%) of total fog water collection as a function of wind direction for the JAS 2018–2019 at Cerro Oyarbide and Alto Patache. Some fog data may not be recorded by our SFCs because of their directional nature

southern winds are twice more frequent and collect almost five times the FW collected by NE winds. Indeed, the south wind component produces nearly 80% of the fog water in AP (Fig. 9). Strong south wind advected fog can produce up to nearly 9 L m^{-2} h^{-1} in AP850, but this is very rare (Figs. 10, 11). S fog events produce high mean water yields (1.3 L m^{-2} h^{-1}, AP850; 0.6 L m^{-2} h^{-1}, AP750) compared to the NE–S and NE events (0.9 L m^{-2} h^{-1}, AP850; 0.4 L m^{-2} h^{-1}, AP750). Max mean AP fog water collection of S events coincide with the late afternoon and early night hours just after strong winds (mean of 5 m s^{-1}, up to 12 m s^{-1}) (Figs. 2, 11). Less strong winds during NE (mean of 4.6 m s^{-1}) and NE–S (mean of 3.2 m s^{-1}) events occurring at other daytimes help explain the difference in fog water yields among different event types. Afternoon orographic fog is ubiquitous in AP and can be linked to maximum fog water collection, which in turn is followed through night as advective fog during a second FW peak (Fig. 3; Table 4). In summary, the S, NE–S and NE fog events occur at different times of the day, last between about 3 and 11 h and occur one or several times per day in AP. Max fog water collection rates occurs under S fog events during the afternoon and early night associated with strong winds.

In Cerro Oyarbide OYA1211, fog presence is linked mostly to NE winds and to a lesser extent SW winds (Figs. 10, 12). Therefore, the NE, SW and SW–NE are the most common fog events, adding 74 events in total for the analyzed period. The most frequent are the NE events (55%) adding 34% of the total fog time recorded. The least common are the SW events (11%), which represent only 3% of the fog time. Both of these fog event types, NE and SW, comprise the shorter event types (mean duration 2 h) compared to the SW–NE events (mean duration 5 h). Rare SW–NE event durations can reach 15 h, longer than the NE and SW extreme events reaching 9–12 h. Therefore, fog occurrence is mostly associated with night–morning time SW–NE events (60% of the total fog time), when most fog water is collected (up to 60%), followed by the night–morning time NE (28%) and mostly daytime SW (12%) event-associated water collection. A common SW–NE event is that starting with late afternoon SW winds and ending with NE winds during night. The same event type can occur between night and morning also. There are no SW–NE events showing a transition from NE to SW winds. Within the SW–NE events, the wind can change iteratively between SW and NE components. The SW and NE winds record the same total time of occurrence in OYA1211, but the SW advected fog produce more than double FW compared to the NE winds. Nonetheless, if the SW and NE advected fog's wind components are compared considering all data (not only the

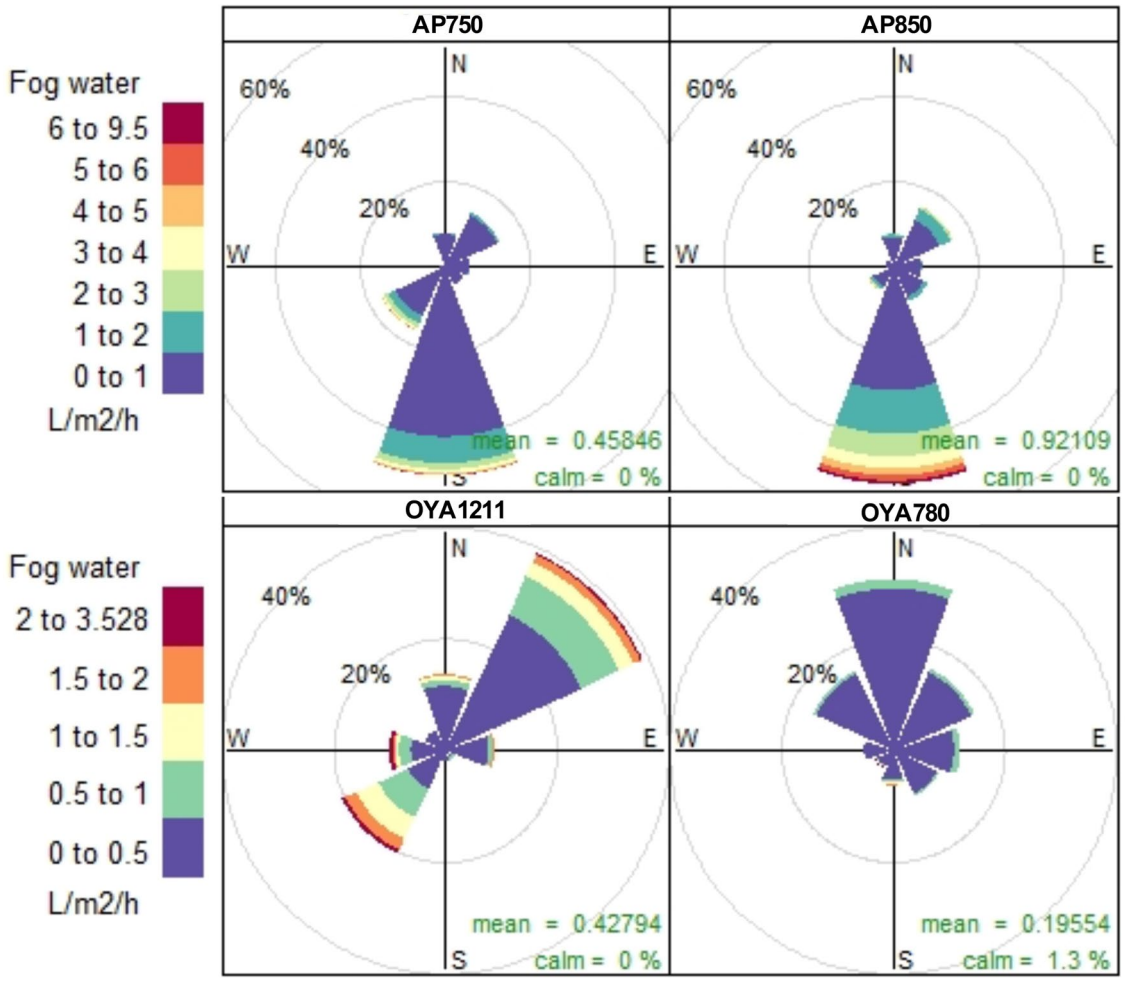

Fig. 10 Frequency of counts of fog water (FW) flux collected per hour as a function of wind direction for the JAS period in 2018–2019 at Cerro Oyarbide and Alto Patache. Some fog data may not be recorded by our SFCs because of their directional nature

SW–NE events), they both produce similar volumes of fog water, adding a total of near 75%, which mostly are collected during late night and early morning hours (Figs. 2, 8). The highest collection means are produced with strong SW and NE (up to 6–8 m s^{-1}) advected fog reaching above 2 L m^{-2} h^{-1} (Figs. 10, 11). In most cases, water collected reaches between 0.1 and 2 L m^{-2} h^{-1} with higher rates more common with SW wind. Mean SW fog events produce high mean water yields (0.8 L m^{-2} h^{-1}) compared to the SW–NE (0.5 L m^{-2} h^{-1}) and NE events (0.4 L m^{-2} h^{-1}). This is partially explained by relatively short and sporadic SW events that deliver, in some cases, relatively high fog water volumes at OYA1211 (Figs. 10, 11). Considering all wind directions, the mean fog water collection is 0.4 l m^{-2} h^{-1} (Fig. 10).

At OYA780, fog presence is linked to multiple wind directions, of which N (30%), NW (15%), NE (15%) and E (10%) are the most common (Fig. 10). N, SE and the SE–N are the most representative fog events, adding 98 events in total. The most frequent are the SE–N events (55%) accounting for 65% of the fog time and the least common are the SE events (5%) representing only 3% of the total fog time. The N events represent the 20% of the total events and the recorded fog time. The SE–N events include higher occurrence of N winds and these are associated with higher FW accumulation compared to SE wind components. These events normally occur during nighttime and end by the morning. The same is true for N and SE events. The mean SE events last only 2 h, in contrast to the SE–N events that have a mean duration of 6 h. N events have intermediate durations (4 and 5 h, respectively). Rare SE–N events durations can reach 16 h, which is longer than the N (12–13 h) and the SE (7 h) extreme events. Most fog water is collected during the N–SE (65%) followed by N events (15–20%) and the SE (2%) events. If the wind components are to be separated, the N winds contribute > 30%, which together with NW and NE winds yield > 60% of total fog water collected

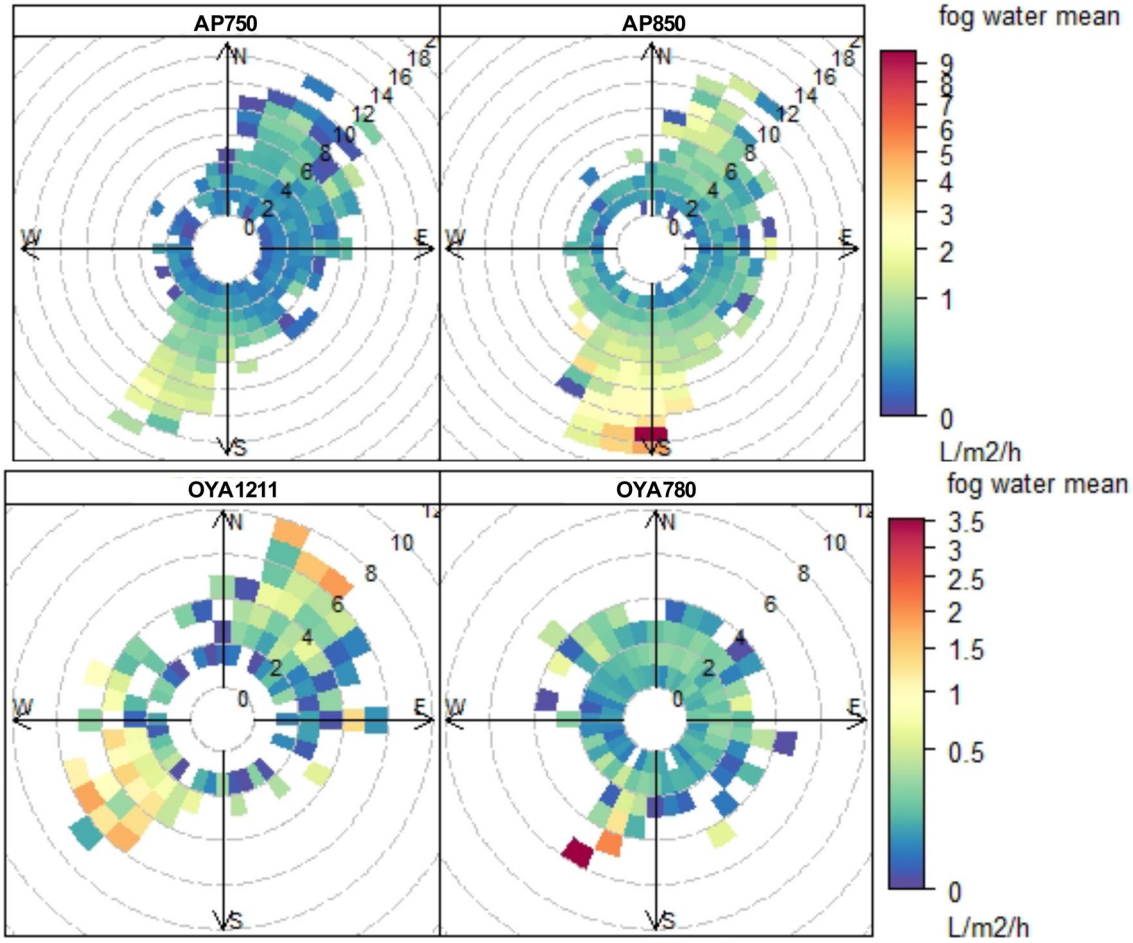

Fig. 11 Mean fog water collection per hour (or fog water flux density) as a function of wind direction and wind speed for the JAS period in 2018–2019 at Cerro Oyarbide and Alto Patache. Some fog data may not be recorded by our SFCs because of their directional nature

at OYA780 (Fig. 9). Interestingly, S, SW and W advected fog only appears to add about 15%. Fog presence and water collection occur for the most part between midnight and early morning, when northward and eastward winds associated with the N and SE–N events predominate (Figs. 8, 11). Virtually no fog events occur through the day in OYA780 when S to W winds predominate. Nonetheless, SW winds produced the highest fog water mean yields (1.8 L m^{-2} h^{-1}), which in the presence of strong winds (4–6 m s^{-1}) yield up 3.5 L m^{-2} h^{-1} near midday (Figs. 11, 12). Nonetheless, mean water yields during a mean fog event reach 0.2 L m^{-2} h^{-1} associated with wind speeds < 3 m s^{-1} (Figs. 10, 11).

Table 4 Daily time of maximum fog presence and fog water collection at each station and the associated mechanisms of origin

Station	Fog presence maximum (day hours)	Fog water maximum (day hours)	Mechanism*
AP750	16–08	16–20	OF, AF
AP850	16–08	16–20	OF, AF
OYA780	00–08	00–08	AF
OYA1211	22–09	23–08	AF

**OF* orographic fog, *AF* advective fog

In summary, the record of fog events can be classified in two fog regimes characterized by a relationship between meteorological variables, such as T, q and wind with the fog water collected. The first one occurs at the AP stations, where fog concentrates in the afternoon when the temperature is low and q the highest, but also under S–SW wind flow that reaches 5–6 m s^{-1}. The second one occurs in OYA stations where fog water concentrates at night and early morning associated with low temperature, low q and variable wind speed and direction (NE-SW in OYA1211 and N in OYA780). Interestingly enough, q is out of phase with fog water collection diurnal cycle in OYA (i.e., the maximum specific humidity does not coincide with max fog water collection) (Fig. 3). The first regime is associated with a blend of local-scale orographic fog plus a larger-scale advective fog, whereas the second fog regime is associated with

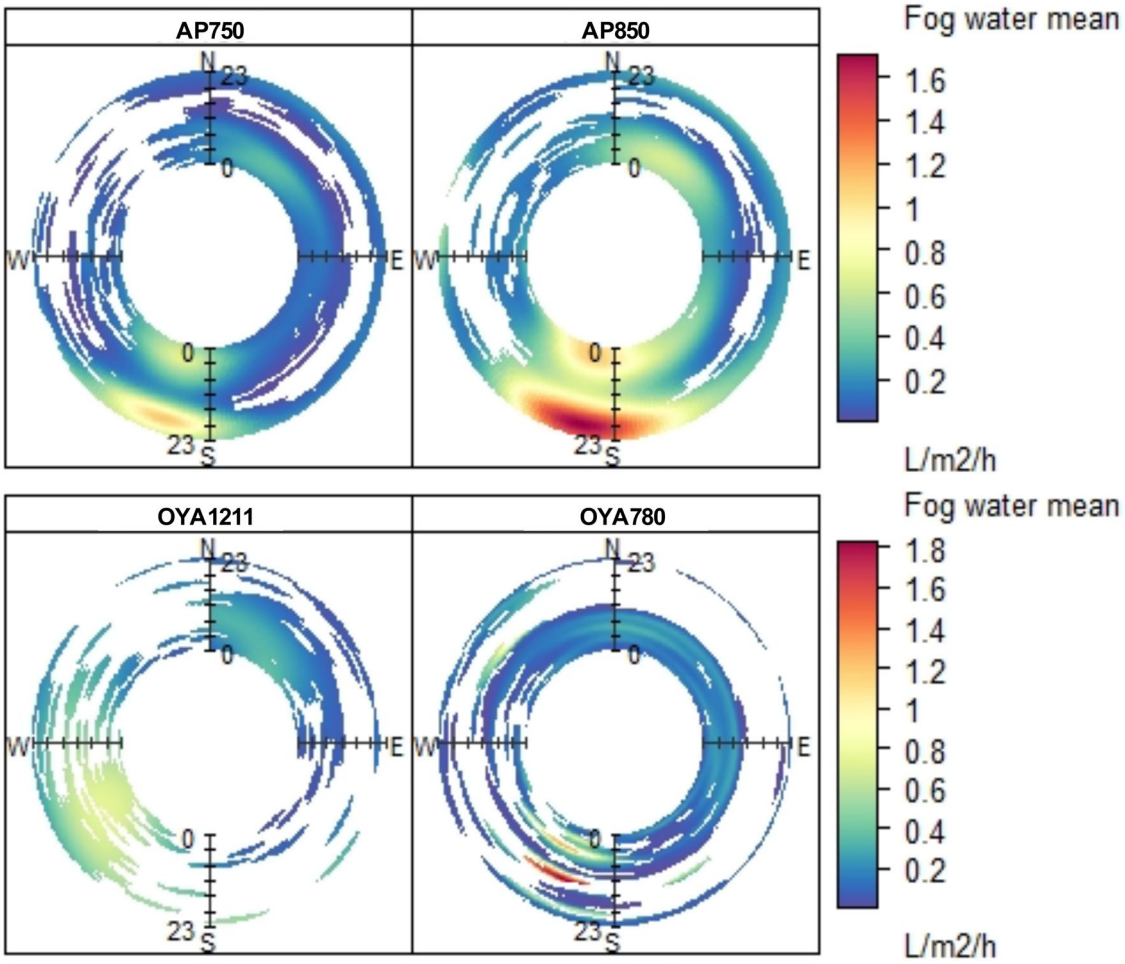

Fig. 12 Fog water collection per hour as a function of wind direction and hour of day for the JAS period in 2018–2019 at Cerro Oyarbide and Alto Patache. Some fog data may not be recorded by our SFCs because of their directional nature

advective fog away from the coastal cliff (Cereceda et al. 2002; Lobos et al. 2018).

MBL during fog events

In this section, we analyze the thermal and moisture state of the MBL during fog events. Then, we compare the occurrence of typical OYA1211 fog events with other stations to assess the geographic expression of MBL during these high-elevation fog scenarios.

As an example of a typical, although rare, fog event that occurs during the JAS and its influence over the *Tillandsia landbeckii* in Cerro Oyarbide area, Fig. 13 shows moisture and thermal variables that characterize the marine boundary layer dynamic during a multiple fog event that occurred between the July 22 and 24, 2019, in OYA1211.

During this event, we observe that fog appears five times. First, it occurs in the night and evening of July 22nd, then evening of the 23rd, then at the night and early morning of July 24th and finally at the late afternoon of July 24th. This multiple fog event shows high fog water collection that reached 3 L m^{-2} h^{-1} at OYA780 and near 2 L m^{-2} h^{-1} at OYA1211. Most of the fog water is collected during the night and early morning. We observe that fog occurred when q has a similar value at both OYA stations (Fig. 13a). Potential temperature (θ) tends to show the same (Fig. 13c). During the three-day composite event, the moisture and thermal gradients between OYA and airport stations were mostly below 0.002 g kg^{-1} m^{-1} and 0.005 K m^{-1}, respectively (Fig. 13b, d). These values indicate the advection of marine air masses in the form of fog reaching 11 km from the coast line and up to 1211 m a. s. l., different to the normal condition in the coastal desert (Fig. 14a, b). The most important fog collection occurred during the night–morning of the 24th, which coincided with SW winds advecting maritime humid air inland (e.g., in the form of fog between OYA780 and OYA1211). Opposite, NE winds predominated the night

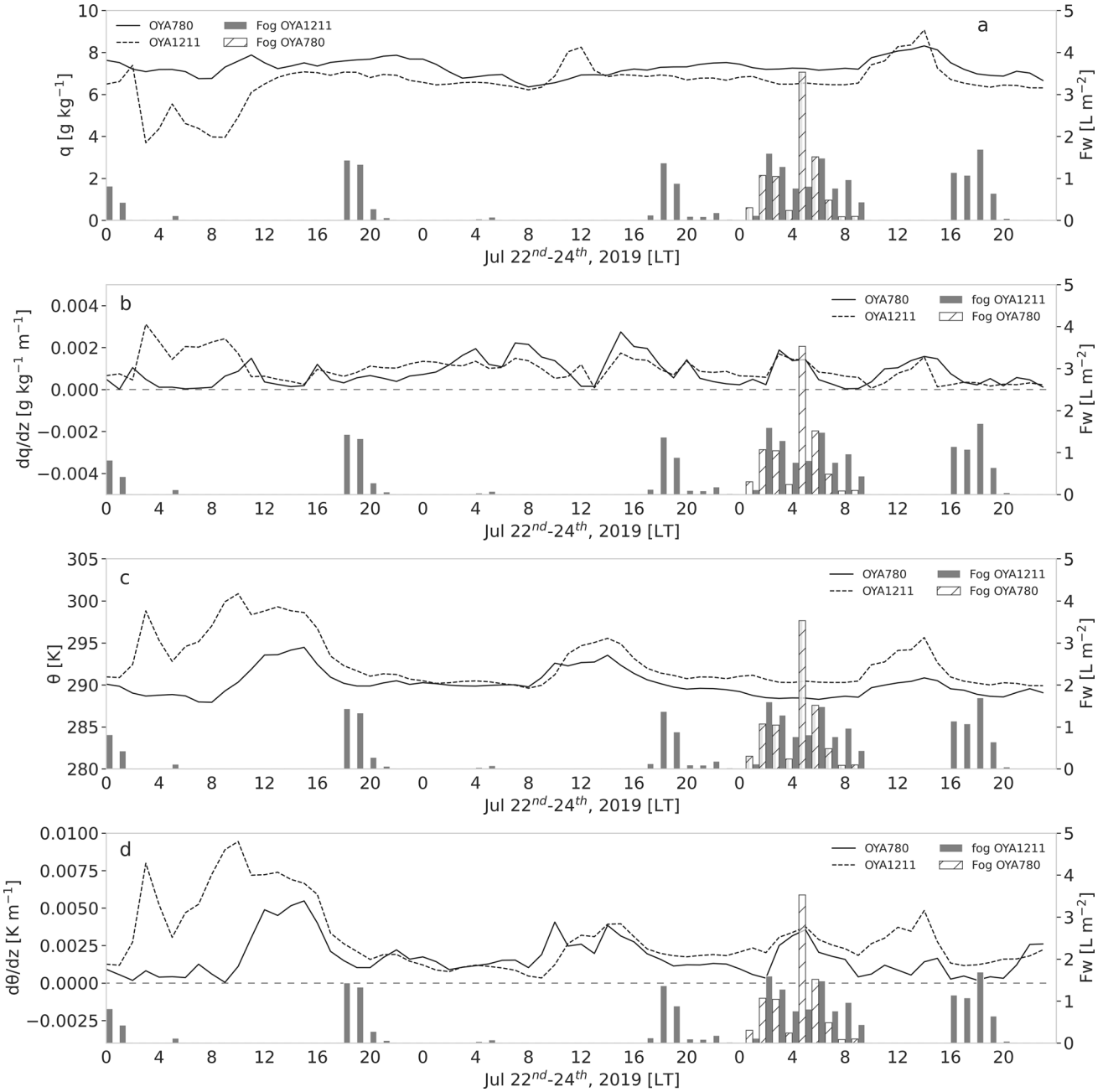

Fig. 13 Composite fog event of the July 22–24, 2019, observed at stations OYA780 and OYA1211. **a** Specific humidity and fog water of OYA780 and OYA1211. **b** Airport-OYA meteo stations moisture gradient (dq/dz) and fog water. **c** Potential temperature and fog water. **d** Airport-OYA meteo stations thermal gradients and fog water. See text for discussion

of the 23rd, when limited water was collected despite similar atmospheric conditions (e.g., air T and wind speed). Interestingly, the night–morning large fog collection on the 24th coincided with larger moisture and thermal gradients than the afternoon events, which indicates that these air masses were less connected to the ones present in the ocean at this time. Nonetheless well-mixed MBL conditions are observed at this time also as high as 1211 m a. s. l. (Fig. 13b, d). One alternative is that the water collection could be explained by dew condensation during this night–morning time. In support of this conclusion, a slower nighttime wind speed could have promoted a thermal and moisture stratification of the marine boundary layer, along with a decrease in temperature, altogether leading to dew condensation on the surface. Recently, del Río et al. (2021a) have recorded advective fog reaching higher than 1000 m a. s. l. only during afternoon time in a nearby site south of Cerro Oyarbide (for JAS 2017), but

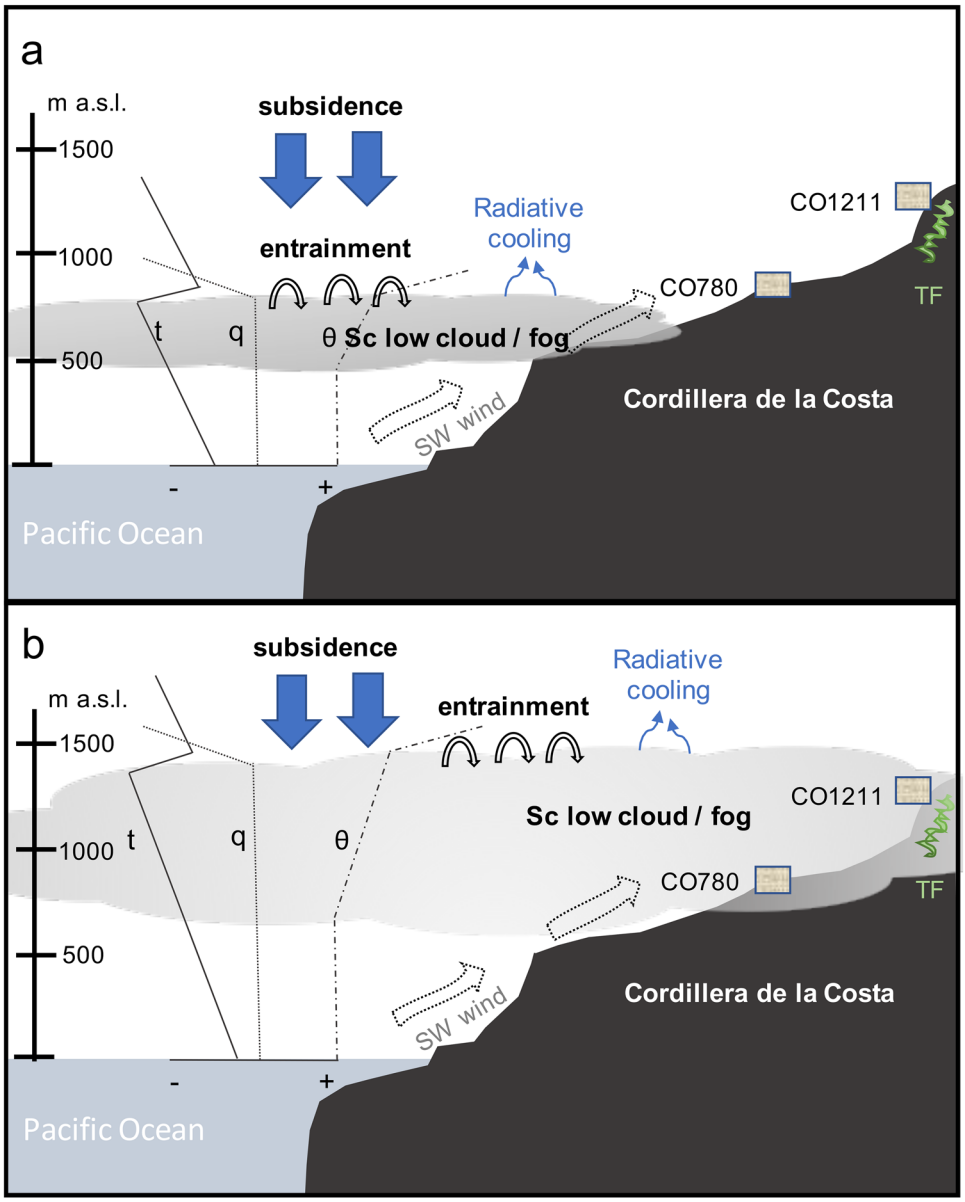

Fig. 14 Contrasting fog scenarios in the costal Atacama fog Desert. Alto Patache is not included because its condition seems abnormal regarding most of the coastal desert land. **a** Normal condition (about 80% of the JAS time) with fog cloud standing below (OYA)780 m a. s. l. and less than 11 km from the coast. **b** Rare fog events (6% of the JAS) reaching at least as high as 1211 m a. s. l., when well-mixed marine air is advected as fog by SW winds > 10 km from the coastline. Fog water is then available for *Tillandsia* uptake during these events. Simultaneous fog presence in OYA1211 and OYA780 is rather a rare condition. TF: Tillandsia fields; t: temperature; q: specific humidity; θ: potential temperature. Modified from Lobos et al. (2018)

not during night–morning time, thus supporting the dew source of water during nights at the heights of the Cordillera de la Costa. Nonetheless, several sources of evidence point to a fog source of the water collected throughout the July 2019 fog event in OYA. First, fog collectors may not actually collect significant enough amounts of dew for the pluviometer to record it. The Raschel mesh does not have significant emissivity nor significant enough mass to accommodate sufficient cooling to promote substantial dew formation. Moreover, the SFCs are mounted vertically, so has an extremely small area directed upward so collect dew. Upward facing material is optimal for the radiative cooling to take place that leads to dew. Therefore, the substantial volumes of water collected during the night of the 24th in both OYA1211 and OYA780 strongly suggest advective fog as the main source. This conclusion does not rule out dew occurring in the Cordillera de la Costa year-round and having a water source influence in *Tillandsia* sp. vegetation (cf., Westbeld et al. 2009).

Multiple long nighttime OYA1211 fog events recorded by our data show a similar anatomy as described for July 22–24, 2019; fog events are preceded by strong (above mean) and pervasive daytime SW winds giving place to low T and high RH preceding the fog. As long as the T stays low (e.g., 5–7 °C) and RH is high, in link with low thermal and moisture vertical gradients, condensation in the form of fog usually occurs through the night and into the morning. If the event is not preceded by a SW wind, it may start when a nocturne switch to this WD occurs, again in association with lowered T, high RH and q values in OYA1211. This

puts special significance on the role of advection in bringing moisture and pushing the MBL high up along the coastal Atacama during fog events into the highlands of the coastal Atacama.

Coincidence of fog occurrence in the four OYA and AP stations is rare, except between OYA1211 and AP stations. In any case, when a long fog event occurs in OYA1211 the lower elevation AP and OYA stations exhibit very high RH (e.g., > 95%) and low T, with or without fog. The temperature decreases with elevation following a typical moist adiabatic T gradient within a well-mixed MBL. The implication then is that fog events at OYA1211, although rare, coincide with the MBL elevation extending at/or above 1.200 m a. s. l., mostly during nighttime. These conditions can last uninterrupted for several days. Synchronic fog presence between 750 and 1250 m a. s. l, although not common, may suggest an extensive high-cloud top making up several hundred-meter-thick fog cloud (cf., Cereceda et al. 2008a; Lobos et al. 2018). Alternatively, this fog scenario could be recording a relatively thin advective fog cloud mantling the topography between 750 and 1200 m a. s. l. The nighttime–dawn occurrence of the fog events corresponds with the proposed high-elevation subsidence thermal inversion base at this time of the day that allows a high-cloud top expanding onto the coastal topography above 1200 m a. s. l (Rutllant et al. 2003; Muñoz et al. 2011). Nonetheless, afternoon events with fog reaching high coastal relief have been also recorded, thus implying a degree of variability of the suggested MBL elevation daily cycle (del Río et al. 2021a; Rutllant et al. 2003).

Implications for the distribution of *Tillandsia landbeckii* ecosystems

The *Tillandsia* landbeckii fields occur along a narrow elevational band between 900 and 1300 m a. s. l. (Pinto et al. 2006; Mikulane et al. 2021) at the boundary between the marine desert and the continental desert by the subsidence inversion base. As shown by the OYA1211 data, the *Tillandsia landbeckii* field at Cerro Oyarbide occurs under extremely arid conditions typical of the higher summits of the Cordillera de la Costa (up to 1250 m a. s. l.) (Fig. 1). Along this elevation range, the RH averages 30% and fog condensation is rare, even during the wetter winter-spring months (only about 6% of the JAS). Moreover, fog is usually absent during summer months (Cereceda et al. 2008a). From our data, we show that fog presence is linked to an upward MBL expansion toward the tillandsia field mostly during nighttime when freshwater uptake of the plants occurs (Fig. 14b). Aside from fog, humid and fresh maritime air expands upwards on a mean daily basis into the tillandsia fields and could represent an extra water input through night and dawn dew (Westbeld et al. 2009). This aspect remains to be quantified in future studies.

The *"tilandsiales"* and the Alto Patache embrace the two fog oases extremes in the hyperarid coastal Atacama. The monospecific *Tillandsia landbeckii* fields contrast with the rich ecosystem found in Alto Patache. Here, together with other coastal fog oases, Muñoz-Schick et al. (2001) recorded a total of 72 vascular plant species, which in turn support a variety of desert fauna. As shown above, the AP site is affected by fog most of the JAS period (73%), but the OYA1211, where the *Tillandsia landbeckii* field at Cerro Oyarbide occurs, only occasional fog occurs (6% of the JAS). This atmospheric condition thus explains the difference between both fog ecosystems and denote the steep moisture and fog gradient from the coast inland. One implication is that tillandsias can survive on very low water input (fog equivalent to 0.7 L/m^2/day as measured on a standard fog collector) at the coastal–inland desert interphase. In fact, the tillandsia cannot survive in foggy settings below 900 m a. s. l, such as in Alto Patache, where higher fog water yields seem to be too much for this plant (e.g., too much water can suffocate them). In OYA780, with similar fog yields as OYA1211 but more regular fog presence under the MBL influence seems also inappropriate for tillandsia to develop.

The deepening of the coastal fog cloud as the MBL cools, along with the lowering of the subsidence inversion base and cloud cover decrease (Schulz et al. 2011a, b; Muñoz et al. 2016; del Río et al. 2021b), could have major impacts on the upper "tilandsiales." As more of these ecosystems are subject to exposure under continental desert conditions and away from the fog and MBL influence, their survival is threatened and elevational ranges will likely contract (cf., Schulz et al. 2011b). Under ongoing climate change in Atacama fog Desert, the continued presence of these singular and unique desert ecosystems cannot be guaranteed in its present distribution. Better modeling along with an increased understanding over the long term of how these ecosystems varied in the past will be needed to provide better estimates of how these will behave under future fog climate scenarios.

Conclusions

The Atacama fog Desert owes its existence to a steep coast–inland climate gradient, which results from the interaction between topography and distinct moist marine and dry continental boundary layers. Data show a dynamic spatial change that embraces rapid and extreme meteorological variability. Important atmospheric changes (e.g., fog presence variability) are controlled by both elevation and distance to coast. Exceptional fog presence–fog water yields in Alto Patache compared to Cerro Oyarbide evidence these

factors but also highlight the importance of site-specific physiographic attributes determining fog in the Atacama (e.g., topographic aspect, geomorphic setting or exposure to dominant fog advected winds).

Afternoon moisture advection from the coast–inland at least as high as 1200 m a. s. l. occurs associated with high potential temperature gradients between the airport and OYA stations, thus supporting the occurrence of afternoon enhanced air subsidence and a low elevation MBL as predicted by the Rutllant Pump model (Rutllant et al. 2003). Strong afternoon SW winds advecting maritime air from the MBL upwards better explain the afternoon increase in moisture high in the Cordillera de la Costa.

Mean small thermal gradients in AP show that this site is frequently within the well-mixed MBL. Higher and variable mean thermal gradients in OYA denote the influence of continental dry desert air 11 km inland and above 780 m a. s. l. Fog presence everywhere occurs associated with low thermal gradients (well-mixed MBL air) and fog absence with high thermal gradients (stratified MBL air).

S and NE wind-driven fog events are common in AP but max fog water collection rates occur with S winds during the afternoon and early night. In Cerro Oyarbide OYA1211, fog presence is linked mostly to NE and SW winds, both of them linked to advective fogs that produce similar volumes of fog water mostly during late night and early morning hours. Fog presence and fog water yields in Alto Patache seem anomalously large compared to most of the coastal desert land.

The *Tillandsia landbeckii* fields at Cerro Oyarbide, together with all such ecosystems that occur along the marine–continental layers interphase between 900 and 1300 m a. s. l. are mostly affected by dry air conditions that are only interrupted by occasionally (6% of the JAS) night-to-morning fog when SW and NE advected low-clouds occur. Here, main fog events lasting several days are preceded by strong daytime SW winds associated with low T and high humidity together with low thermal and moisture vertical gradients. Both diurnal and mostly nocturnal fog water is then available for *Tillandsia* uptake during these events. Because summer is mostly fog-free, JAS fog should be a main source of water for the *Tillandsia* ecosystems in this dry limit environment, although dew cannot be ruled out.

The Tillandsia geographic distribution seems to sensitively respond both to elevation and distance to the coast. It seems highly adapted to a narrow altitudinal band (900–1300 m a. s. l.) and near 10 km inland, where air is mostly dry and fog water input is very low (fog equivalent to 0.7 L m^{-2} day^{-1}). Below 900 m a. s. l., the MBL influence as moist air and more frequent fog presence do not allow tillandsia survival. High fog water yields as those in Alto Patache (fog equivalent to 12.4 L m^{-2} day^{-1}) has the same effect. It is then expected that the ongoing fog belt change (Muñoz et al. 2016; del Río et al. 2021b) results in a contraction of tillandsia fields.

Acknowledgements We are very grateful to the Centro UC Desierto de Atacama, Estación Atacama UC_Alto Patache and Constanza Vargas for field support. This research was funded by the Vicerrectoría de Investigación Pontificia Universidad Católica de Chile and Agencia Nacional de Investigación y Desarrollo (ANID-Chile) grant ELAC2015/T01-0872. Station AP750, meteorological measurements at Iquique Airport and work of J.H. Schween were funded by the Collaborative Research Centre 1211 "Earth—Evolution at the Dry Limit" of the German Research Foundation (DFG SFB 1211, Projektnummer 268236062). Camilo del Río would like to thank the ANID/FONDECYT Iniciación grant No 11200789. We also thank two anonymous reviewers for valuable comments improving the quality of this paper.

Funding Vicerrectoría de Investigación Pontificia Universidad Catolica de Chile. Agencia Nacional de Investigación y Desarrollo (ANID-Chile) international Grant ELAC2015/T01-0872, FONDECYT 11200789. Deutsche Forschungsgemeinschaft (DFG, German Research Foundation) Collaborative Research Centre 1211 "Earth—Evolution at the Dry Limit" (SFB 1211, Projektnummer 268236062).

Declarations

Conflict of interest The authors declare no conflict of interest.

References

ASF DAAC (2011) ALOS PALSAR_Radiometric_Terrain_Corrected_high_res; Available at: https://asf.alaska.edu/. Accessed 22 Sep 2020

Borthagaray AI, Fuentes MA, Marquet PA (2010) Vegetation pattern formation in a fog-dependent ecosystem. J Theor Biol 265:18–26. https://doi.org/10.1016/j.jtbi.2010.04.020

Cereceda P, Larraín H, Osses P, Schemenauer RS, Farías M, Lagos M (2002) Radiation, advective and orographic fog in the Tarapacá region, Chile. Atmos Res 64:262–271. https://doi.org/10.1016/S0169-8095(02)00097-2

Cereceda P, Larraín H, Osses P, Farías M, Egaña I (2008a) The spatial and temporal variability of fog and its relation to fog oases in the Atacama Desert, Chile. Atmos Res 87:312–323. https://doi.org/10.1016/j.atmosres.2007.11.012

Cereceda P, Larraín H, Osses P, Farías M, Egaña I (2008b) The climate of the coast and fog zone in the Tarapacá Region, Atacama Desert, chile. Atmos Res 87:301–311. https://doi.org/10.1016/j.atmosres.2007.11.011

del Río C, García JL, Osses P, Zanetta N, Lambert F, Rivera D, Siegmund A, Wolf N, Cereceda P, Larraín H, Lobos F (2018) Enso influence on coastal fog-water yield in the Atacama Desert, Chile. Aerosol Air Qual Res 18:127–144. https://doi.org/10.4209/aaqr.2017.01.0022

del Río C, Lobos F, Siegmund A, Tejos C, Osses P, Huaman Z, Meneses JP, García JL (2021a) GOFOS, ground optical fog observation system for monitoring the vertical stratocumulus-fog cloud dynamic in the coast of the Atacama Desert, Chile. J Hydrol 597:126190. https://doi.org/10.1016/j.jhydrol.2021.126190

del Río C, Lobos F, Latorre C, Koch MA, García JL, Osses P, Lambert F, Alfaro F, Siegmund A (2021b) Spatial distribution and interannual variability of coastal fog and low clouds cover in the

hyper-arid Atacama Desert and implications for past and present *Tillandsia landbeckii* ecosystems. Pl Syst Evol (**in press**)
Duynkerke PG, Zhang HQ, Jonker PJ (1995) Microphysical and turbulent structure of nocturnal stratocumulus as observed during ASTEX. J Atmosp Sci 52:2763–2777
Farías M, Cereceda P, Osses P, Larraín H (2005) Comportamiento espacio temporal de la nube estratocúmulo, productora de niebla en la costa del desierto de Atacama (21° lat. S., 70° long W.) durante un mes de invierno y otro de verano. Invest Geogr 56:43–61
Fuenzalida H (1950) Clima. In: Corporación de Fomento de la Producción (ed) Geografía Económica de Chile. Vol I. Imprenta Universitaria, Santiago de Chile, pp 199–281
Garreaud R, Barichivich J, Christie D, Maldonado A (2008) Interannual variability of the coastal fog at Fray Jorge relict forests in semiarid Chile. J Geophys Res 113:G04011. https://doi.org/10.1029/2008JG000709
González AL, Fariña JM, Pinto R, Pérez C, Weathers KC, Armesto JJ, Marquet PA (2011) Bromeliad growth and stoichiometry: responses to atmospheric nutrient supply in fog-dependent ecosystems of the hyper-arid Atacama Desert, Chile. Oecologia 167:835–845. https://doi.org/10.1007/s00442-011-2032-y
Houston J, Hartley AJ (2003) The central andean west-slope rainshadow and its potential contribution to the origin of hyper-aridity in the Atacama desert. Int J Climatol 23:1453–1464. https://doi.org/10.1002/joc.938
Jaeschke A, Böhm C, Merklinger FF, Bernasconi SM, Reyers M, Kusch S, Rethemeyer J (2019) Variation in $\delta^{15}N$ of fog-dependent *Tillandsia* ecosystems reflect water availability across climate gradients in the hyperarid Atacama Desert. Glob Planet Change 183:103029. https://doi.org/10.1016/j.gloplacha.2019.103029
Koch MA, Kleinpeter D, Auer E, Siegmund A, del Río C, Osses P, García JL, Marzol MV et al (2019) Living at the dry limits: ecological genetics of Tillandsia landbeckii lomas in the Chilean Atacama Desert. Pl Syst Evol 305:1041–1053. https://doi.org/10.1007/s00606-019-01623-0
Koch MA, Stock C, Kleinpeter D, del Río C, Osses P, Merklinger FF, Quandt D, Siegmund A (2020) Vegetation growth and landscape genetics of *Tillandsia* lomas at their dry limits in the Atacama Desert show fine-scale response to environmental parameters. Ecol Evol 10:13260–13274. https://doi.org/10.1002/ece3.6924
Latorre C, González AL, Quade J, Fariña JM, Pinto R, Marquet PA (2011) Establishment and formation of fog-dependent Tillandsia landbeckii dunes in the Atacama Desert: Evidence from radiocarbon and stable isotopes. J Geophys Res 116:G03033. https://doi.org/10.1029/2010JG001521
Lobos Roco F, Villa-Guerau de Arellano J, Pedruzo-Bagazgoitia X (2018) Characterizing the influence of the marine stratocumulus cloud on the land fog at the Atacama Desert. Atmos Res 214:109–120. https://doi.org/10.1016/j.atmosres.2018.07.009
Mikulane S, Siegmund A, Koch MA, del Río C, Osses P, García JL (2021) Semi-automatic detection of Tillandsia fields based on satellite data in the Tarapacá Region (Atacama Desert, Northern Chile). Pl Syst Evol 307(**in review**)
Muñoz RC, Garreaud RD (2005) Dynamics of the Low-level jet off the west coast of subtropical South America. Mon Weather Rev 133:3661–3677. https://doi.org/10.1175/MWR3074.1
Muñoz RC, Zamora RA, Rutllant JA (2011) The coastal boundary layer at the eastern margin of the southeast pacific (23.48°S, 70.48°W): cloudiness-conditioned climatology. J Clim 24:1013–1033. https://doi.org/10.1175/2010JCLI3714.1
Muñoz R, Quintana J, Falvey M, Rutllant J, Garreaud RD (2016) Coastal clouds at the eastern Margin of the southeast Pacific: climatology and trends. J Clim 29:4525–4542. https://doi.org/10.1175/JCLI-D-15-0757.1
Muñoz-Schick M, Pinto R, Mesa A, Moreira-Muñoz A (2001) "Oasis de Neblina" en los cerros costeros del sur de Iquique, región de Tarapacá, Chile, durante el evento El Niño 1997-1998. Revista Chilena de Historia Natural 74:389–405
Pinto R, Barria I, Marquet PA (2006) Geographical distribution of Tillandsia lomas in the Atacama Desert, northern Chile. J Arid Environm 65:543–552. https://doi.org/10.1016/j.jaridenv.2005.08.015
Regalado CM, Ritter R (2016) The design of an optimal fog water collector: a theoretical analysis. Atmos Res 178–179:45–54. https://doi.org/10.1016/j.atmosres.2016.03.006
Rutllant JA, Fuenzalida H, Torres R, Figueroa D (1998) Interacción océano atmósfera tierra en la región de Antofagasta (Chile, 22°S): Experimento DICLIMA. Revista Chilena Hist Nat 71:405–427
Rutllant JA, Fuenzalida H, Aceituno P (2003) Climate dynamics along the arid northern coast of Chile: The 1997–1998 dinámica del clima de la región de Antofagasta (diclima) experiment. J Geophys Res 108:D17. https://doi.org/10.1029/2002JD003357
Schween JH, Hoffmeister D, Loehnert U (2020) Filling the observational gap in the Atacama Desert with a new network of climate stations. Global Planet Change 184:103034. https://doi.org/10.1016/j.gloplacha.2019.103034
Schemenauer RS, Cereceda P (1994) A proposed standard fog collector for use in high elevation regions. J Appl Meteorol 33:1313–1322
Schulz N, Boisier JP, Aceituno P (2011a) Climate change along the arid coast of northern Chile. J Climatol 32:1803–1814. https://doi.org/10.1002/joc.2395
Schulz N, Aceituno P, Richter M (2011b) Phytogeographic divisions, climate change and plant dieback along the coastal desert of northern Chile. Erdkunde 65:169–187. https://doi.org/10.3112/erdkunde.2011.02.05
Voigt C, Klipsch S, Herwartz D, Chong G, Staubwasser M (2020) The spatial distribution of soluble salts in the surface soil of the Atacama Desert and their relationship to hyperaridity. Global Planet Change 184:103077. https://doi.org/10.1016/j.gloplacha.2019.103077
Weischet W (1975) Las condiciones climáticas del desierto de Atacama como desierto extremo de la Tierra. Revista Geogr Norte Grande 1:363–373
Westbeld A, Klemm O, Griessbaum F, Strater E, Larraín H, Osses P, Cereceda P (2009) Fog deposition to a Tillandsia carpet in the Atacama Desert. Ann Geophys 27:3571–3576. https://doi.org/10.5194/angeo-27-3571-2009